Turun yliopisto
University of Turku

NONSPECIFIC BINDING IN SANDWICH-TYPE-IMMUNOASSAYS UTILIZING NANOPARTICULATE LABELS

Tuomas Näreoja

ACADEMIC DISSERTATION
To be presented, with assent of the Medical Faculty of the University of Turku,
for public examination in Auditorum Osmo Järvi, Kiinamyllynkatu 10, ground floor,
on August 8th 2014, at 12 o'clock noon

TURUN YLIOPISTON JULKAISUJA – ANNALES UNIVERSITATIS TURKUENSIS
Sarja - ser. D osa - tom. 1123 | Medica - Odontologica| Turku 2014

Turun yliopisto
University of Turku

NONSPECIFIC BINDING IN SANDWICH-TYPE-IMMUNOASSAYS UTILIZING NANOPARTICULATE LABELS

Tuomas Näreoja

TURUN YLIOPISTON JULKAISUJA – ANNALES UNIVERSITATIS TURKUENSIS
Sarja - ser. D osa - tom. 1123 | Medica - Odontologica | Turku 2014

University of Turku

Faculty of Medicine

Institute of Biomedicine

Department of Cell Biology and Anatomy, Laboratory of Biophysics and Medicity laboratories

University of Turku Doctoral Programme of Molecular Medicine (TuDMM)

National Doctoral Programme in Informational and Structural Biology (ISB).

Supervised by

Professor Pekka Hänninen, Ph.D.

Laboratory of Biophysics

Department of Cell Biology and Anatomy

University of Turku,

Turku, Finland

Docent Harri Härmä Ph.D.

Laboratory of Biophysics

Department of Cell Biology and Anatomy

University of Turku,

Turku, Finland

Reviewed by

Docent Kristiina Takkinen, Ph.D.

Immunotechnology

VTT

Espoo, Finland

Professor Niko Hildebrandt Ph.D.

Nano Bio Photonics

Institute d'Electronique Fondamentale

Université Paris-Sud

Orsay, Paris, France

Opponent

Professor Hans Tanke, Ph.D.

Department of MElecular Cell Biology

Leiden University Medical Center

Leiden, The Netherlands

The originality of this thesis has been checked in accordance with the University of Turku quality assurance system using the Turnitin Originality Check service.

ISBN 978-951-29-5796-5 (PRINT)
ISBN 978-951-29-5797-2 (PDF)
ISSN 0355-9483

Suomen Yliopistopaino Oy, Juvenes Print, Turku, Finland 2014

Tuomas Näreoja

Nonspecific binding in sandwich-type immunoassays utilizing nanoparticulate labels

Department of Cell Biology and Anatomy, Laboratory of Biophysics, Institute of Biomedicine, Faculty of Medicine in University of Turku, Finland.
University of Turku Doctoral Programme of Molecular Medicine (TuDMM) and the National Doctoral Programme in Informational and Structural Biology (ISB)

Annales Universiatis Turkuensis, Medica – Odontologica Painosalama Oy, Turku, Finland 2014

ABSTRACT

Nanoparticle labels have proved to possess high specific activity and even single binding events can be observed due to the extremely intense luminescence of the particles as compared to molecular labels. This is mainly due to a high concentration of label units within a nanoparticle, novel particle materials or high absorption cross-section. However, higher sensitivity has not been achieved solely by improving the labels. In addition, a bioconjugate nanoparticle with a diameter of 90 nm typically has around 100 binding sites, when it is coated with whole antibodies. Hence, the avidity of a nanoparticle label coated with multiple antibodies has been shown to exceed that of a soluble, labeled antibody. More than ten-fold higher affinity constants have been measured for bioconjugate nanoparticles than the respective molecular antibodies. These factors have led to the improved sensitivity and ten- to hundred-fold lower detection limits. Due to the high specific activity of the nanoparticle labels, nonspecific binding has become an important sensitivity-limiting factor of nanoparticle-based assays in a variety of applications in diagnostics and drug development. They seem also to be more susceptible to matrix effects in the assay.

We have demonstrated general principles that take into account the specific considerations involved with nanoparticulate labels to provide the optimal assay configuration. The use of large, stabile and flexible binders coated to nanoparticle surface are preferred over smaller that would potentially give rise to a more dense coating. The solid phase is better accessible to nanoparticles and less prone to denature when an adaptor molecule is used to orient a dense layer of binders, such as Fab-fragments. These, in combination with controlling the association time by liquid flow to disallow association of nonspecific binding could be the optimal strategy to reduce the undesired nonspecific background signal in immunoassays utilizing bioconjugate nanoparticles. Furthermore, in the preparation of nanoparticles the relatively slow exchange of loosely bound adsorbed proteins dictates the optimal sequence in introducing the nanoparticulate labels to the assay matrix. Finally, we demonstrate an assay that was able to detect 60 nIU/L TSH concentration, a nearly 100-fold decrease in the lowest limit of detection in comparison to 4th generation TSH assay.

Keywords: medical diagnostics, immunoassay, nanoparticle labels, nonspecific binding, time-resolved luminescence

Tuomas Näreoja

Epäspesifisien sitoutumisreaktioiden syyt ja niiden vähentäminen nanopartikkelileimoja hyödyntävissä kaksikohtaisissa immunomäärityksissä

Solubiologia ja anatomia, Biofysiikan laboratorio, Biolääketieteen laitos, Lääketieteellinen tiedekunta, molekyylilääketieteen tohtoriohjelma (TuDMM) ja kansallinen bioinformatiikan ja rakennebiologian tutkijakoulu (ISB), Turun Yliopisto, Turku.

Annales Universiatis Turkuensis, Medica – Odontologica Painosalama Oy, Turku 2014

TIIVISTELMÄ

Fluoresenssisignaalia käyttävissä immunomäärityksissä vasta-ainepäällysteisistä nanopartikkelileimoista saadaan erittäin voimakas signaali ja jopa yksittäisten molekyylien havainnoiminen biologisista näytteistä on mahdollista. Yhteen nanopartikkeliin voidaan sisällyttää kymmeniätuhansia tai jopa miljoonia yksittäisiä leimamolekyylejä, ne voidaan valmistaa valoa tehokkaasti absorboivasta materiaalista ja ne suojaavat virittyneitä leimamolekyylejä sivureaktiolta. Nanopartikkeleilla pinta-alan suhde tilavuuteen on hyvin suuri. Yhden 90 nm nanopartikkelein pinnalle voidaan kiinnittää yli sata sitojaa, jolloin leiman sitoutumisvakio kasvaa tyypillisesti yli kymmenkertaiseksi verrattuna tavanomaiseen molekulaariseen leimattuun vasta-aineeseen. Nämä ominaisuudet ovat mahdollistaneet äärimmäisen herkkien ja tarkkojen diagnostisien testien kehittämisen. Nanopartikkeliteknologiaa hyödyntävien testien määritysraja voi olla jopa sata kertaa matalammalla pitoisuudella kuin perinteisen testin. Valitettavasti nanopartikkelileimojen suuri pinta-ala on myös lisännyt niiden ei-toivottua epäspesifistä sitoutumista. Ne kärsivät enemmän myös näytematriisin aiheuttamista ongelmista. Nämä seikat ovat osaltaan estäneet nanopartikkelileimojen laajamittaisemman käytön.

Tässä väitöskirjatutkimuksessa olemme selvittäneet nanopartikkelileimojen sitoutumismekanismeja, sitoutumiseen vaikuttavia vasta-aineiden kiinnittämismalleja, pyrkineet vähentämään ei-toivottua epäspesifistä sitoutumista ja luomaan tarkemman sekä herkemmän diagnostisen määrityksen aivolisäkkeen tuottamalle tyreotropiinille. Tutkimuksemme mukaan paras mahdollinen vasta-aineyhdistelmä oli nanopartikkeliin kiinnitetty kokonainen monoklonaalinen vasta-aine ja mikroreaktioastiaan kiinnitettynä toimi parhaiten streptavidiinipinnalle kiinnitetty paikkaspesifisesti biotinyloitu Fab-tyyppinen vasta-aineen osa. Havaitsimme myös, että suurin ero spesifisen ja epäspesifisen sitoutumisen välillä ei ollut sitoutumisvoimakkuudessa vaan sitoutumisnopeus oli ratkaisevasti erottava tekijä. Siksi mikroreaktioastian toiminnallisen pinnan tuli kattaa vain pieni osa kokonaispinta-alasta, jotta nanopartikkelin sitoutumisaikaa voitiin rajoittaa sekoitusnopeutta nostamalla. Yhtälailla tärkeää oli antaa nanopartikkelileiman pinnalle adsorboituvien proteiinien saavuttaa reaktiotasapaino ennen kuin määritys käynnistettiin. Onnistuimme mittaamaan tyreotropiinipitoisuuden 60 nIU/L perustamalla määrityksen kehitys havaintoihimme nanopartikkelileimojen sitoutumismekanismeista.

Avainsanat: immunomääritys, nanopartikkelileima, aikaerotteinen fluoresenssi, epäspesifinen sitoutuminen

TABLE OF CONTENTS

ABBREVIATIONS

Ab	Antibody
AFM	Atom force microscope
Ag	Antigen
A/V-ratio	Area-to-volume ratio
Bg	Background signal
BgG	Nonspecific bovine γ-globulin
BLI	Biolayer interferometry
BSA	Bovine serum albumin
CV%	Coefficient of variation
DL	Double layer (of charged ions)
DTPA	Diethylene triamine pentaacetic acid
EDC	1-ethyl-3-(3-dimethylaminopropyl) carbodiimide hydrochloride
ELISA	Enzyme-linked immunosorbent assay
Fab	Fragmented antibody, includes both light-chain domains and respective heavy-chain domains
Fc-domain	Constant heavy-chain domain of an antibody
FDC	Force-distance cycle
FIA	Fluoroimmunoassay
FRET	Fluorescence resonance energy transfer
FS	Force spectroscopy
HAB	Human autoantibody
HAMA	Human anti-mouse antibodies
HBT	Heterophile (antibody) blocking tubes
K_d	Equilibrium binding constant
LLD	The lowest limit of detection
LOQ	The lowest limit of quantitation

Mab	whole monoclonal antibody
MPUF	Most probable unbinding force
NHS	N-hydroxysuccinimide
PDF	Probability density function
PSA	Prostate-specific antigen
S/B	signal-to-background ratio
scFv	Single-chain hypervariable domain of an antibody
SD	Standard deviation
SDS	Sodium dodecyl sulphate
S_{LLD}	Signal at LLD
S_{LOQ}	Signal at LOQ
TR-FIA	Time-resolved fluoroimmunoassay
TSH	Thyroid stimulating hormone
UCP	Up-converting phosphor
UV	Ultraviolet

LIST OF ORIGINAL PUBLICATIONS

I. Tuomas Näreoja, Markus Vehniäinen, Urpo Lamminmäki, Pekka E. Hänninen, and Harri Härmä. 2009. "Study on Nonspecificity of an Immuoassay Using Eu-Doped Polystyrene Nanoparticle Labels." *Journal of Immunological Methods* 345 (1-2): 80–89.

II. Tuomas Näreoja, Anni Määttänen, Jouko Peltonen, Pekka E. Hänninen, and Harri Härmä. 2009. "Impact of Surface Defects and Denaturation of Capture Surface Proteins on Nonspecific Binding in Immunoassays Using Antibody-Coated Polystyrene Nanoparticle Labels." *Journal of Immunological Methods* 347 (1-2): 24–30.

III. Tuomas Näreoja, Andreas Ebner, Hermann J Gruber, Barbara Taskinen, Ferry Kienberger, Pekka E Hänninen, Vesa P Hytönen, Peter Hinterdorfer, and Harri Härmä. 2014. "Kinetics of Bioconjugate Nanoparticle Label Binding in a Sandwich-Type Immunoassay." *Analytical and Bioanalytical Chemistry* 406 (2): 493–503.

IV. Tuomas Näreoja, Urpo Lamminmäki, Harri Härmä and Pekka E. Hänninen 2014. "Super-sensitive time-resolved fluoroimmunoassay for TSH utilizing europium(III) nanoparticle labels with reduced nonspecific binding." Submitted manuscript

In addition some unpublished data is presented.

1. INTRODUCTION

Bioaffinity assays have become a predominant method of analysis in diagnostics and drug development because of their sensitivity, selectivity and versatility. After their invention in the late 1950's [1] and [2], a number of refinements and improvements have been introduced. The non-competitive or sandwich-type immunoassays [3] and [4] that hold potential for higher sensitivity and a wider dynamic range [5], [6] and [7] ultimately facilitate detection of single molecules. Such sensitivities, however, required advances throughout the entire field of bioanalysis. The sandwich-type immunoassays are to this day widely applied in clinical diagnostics. They provide the majority of the most sensitive assays, but require multiple steps and washes.

The first bioaffinity assays used radiolabelled polyclonal antibodies as reporter molecules. Radiolabels are still wildly applied in assays where the binder is small (≤1 kDa) and conjugation of the binder to a label of corresponding or even larger size would render the assay non-functional. Non-isotopic labels have largely replaced the radiolabels due to economic, shelf-life issues, environmental and work safety aspects. While the radiolabels cause minimal disturbance for binding of haptens and are widely used as a label in small-ligand binding assays, they cannot be effectively utilised in multianalyte assays nor provide the sensitivities delivered by photoluminescent and enzymatic labels [6]. The work on non-isotopic labels was pioneered by the development of polarimetric immunoassays [8] and [9], ELISA (enzyme-linked immunosorbent assay) [10] and [11] and FIA/IFMA (fluoroimmunoassay/immunofuorometric assay) [12]. However, antibodies labelled with fluorescent compounds were utilised much earlier in immunofluorescence method for detection of pneumococci in tissue slices under fluorescence microscope [13] and [14]. FIAs, on the other hand, have problems related to scattered excitation light and autofluorescence emitting from lab ware and biological materials [15]. Among successful FIA-systems currently in use are Cobas (Roche), ARCHITECT (Abbot Diagnostics), AVIDA (Siemens), dissociation enhanced lanthanide fluoroimmunoassay (DELFIA) (PerkinElmer), time-resolved amplified cryptate emission (TRACE) (Thermo Scientific) and HTRF-technology (Cisbio assays).[16]

Nanoparticle labels have proved to possess high specific activity and even single binding events can be observed due to the extremely intense luminescence of the particles as compared to molecular labels [17], [18], [19] and [20]. The use of lanthanide incorporated nanoparticles was pioneered by Frank and Sundberg preparing the first polystyrene nanoparticles embedded with thenoyltrifluoroacetone lanthanide-chelate complexed with tri-n-octylphosphine oxide in the late 1970' [21]. The advantages arise from the high concentration of label units within a nanoparticle, novel particle materials or high absorption cross-section [22].

The higher signal yield of labels is not the only property of the nanoparticle labels that improves immunoassay sensitivity. In addition, avidity of a nanoparticle label coated with multiple antibodies has been shown to exceed affinity of the soluble, labeled antibody. More than ten-fold higher affinity constants have been measured for bioconjugated nanoparticles than the respective molecular antibodies [23]. These three factors have mainly led to improved sensitivity. Ten- to hundred-fold lower detection limits have been measured [24]. Due to the high specific activity of the nanoparticle labels, nonspecific binding has become an important sensitivity-limiting factor of nanoparticle-based assays in a variety of applications in diagnostics and drug development [25].

Nanoparticle labels are large in size when compared to molecular labels with size variation typically from ten to hundreds of nanometers. The probability for successful binding has increased together with multiple binding sites, but the same avidity-effect applies to nonspecific binding. Increase in both association rate constants and slower diffusion [26] markedly change the kinetics in sandwich-type immunoassays utilizing bioconjugate nanoparticles labels. The large size of the labels may promote nonspecific binding to concave surfaces. If there are uneven surfaces and cavities on the solid-phase surface, they could potentially retain nanoparticles due to their larger surface area available for interactions. Also other features present on polystyrene surfaces or denatured antibodies in the biofunctionalized layer have been suggested to induce patches with alternating binding properties, which could lead to nonspecific binding of nanoparticle labels or an uneven antibody coating of the polystyrene surface [27] and [28].

Another paradigm of reducing nonspecific interactions in sandwich immunoassays relies on fragmentation of antibodies to single-chain Fv (scFv) or Fab fragments [29] and [30]. The fragments have their antigen recognition sites, but lack the Fc-part and they have commonly been produced by recombinant DNA technologies [31]. They are smaller in size and they lack the parts not involved in antigen recognition, such as the Fc-part. The benefits of such fragments are to provide a more dense coating binding sites, an optimized binding to small antigens [32] and elimination Fc-part related cross-reactivity, e.g. complement and glycosylation related interactions [33]. To produce a dense coating on a nanoparticle typically site-specifically oriented molecules are utilized. The site specificity can be obtained by inserting certain amino acids to generate e.g. thiols or specific protein domains e.g. biotin carboxyl carrier protein [34]. However, some of these gains come at the expense of stability of the antibody fragments, their partial denaturation can generate more nonspecific binding or loss of binding sites over time [30].

The field of *in vitro* diagnostics strives to provide clinicians more information with better precision and accuracy in order for patients to get the best available treatment as soon as possible [35]. This thesis weighs the benefits and disadvantages of different techniques to create general trends for future immunoassay development and to further decrease the limit of detection. However, precision and accuracy are often problematic in a number of test formats and small changes in trends cannot be detected. Therefore, more powerful tools are required to quantitatively detect low analyte concentrations and trend reversals due to intervention therapy. In serum, matrix related interference, e.g. elevated nonspecific binding, autoantibodies, polyanions and human anti-mouse antibodies (HAMA), often hamper precise measurements. Here we demonstrate the effects that the conceptual findings have to the performance of a biologically relevant TSH assay in sandwich-type immunoassays utilizing nanoparticle labels. The optimized europium(III) nanoparticle labeling technology is shown to improve the LLD by nearly two orders of magnitude to 60 nIU/L that equals to 450 aM [36].

2. REVIEW OF THE LITERATURE

2.1. Immunoassays

Competitive, heterogeneous

Competitive or reagent-limited immunoassays are categorized by competition from binding sites between non-labeled sample molecules and labeled detector molecules. First immunoassays developed were competitive immunoassays [1]. In the classical case measured signal intensity correlates inversely to the concentration of sample molecules. The displaced and unbound labeled detector molecules are removed by washing, and subsequently signal intensity is read from the capture surface. In such cases, the dynamic range is constricted to two orders of magnitude at best and LLD usually higher than in non-competitive immunoassays. [7]

Competitive, homogeneous

In homogenous assays, the modulation of output signal is recorded as a result of sample molecule binding. In terms of fluorescence signal modulation can be detected by measuring e.g. anisotropy [37], lifetime or wavelength of emission (FRET-signal) [38]. Depending on the setup the signal resulting from displacement of the labeled sample molecule analog, can be either ascending or descending. Competitive homogenous immunoassays are chosen when sample molecules have low molecular weight or the assay needs to be especially simple to execute. [7]

Non-competitive, heterogeneous

Non-competitive reagent excess immunoassays are the most common immunoassay type, and also known as two-site or sandwich-type immunoassays (Figure 1). In this format, the sample molecule is recognized from two independent sites, from one to capture it to the solid-phase and from another to visualize it with a labeled detector. Thus, the signal intensity directly proportional to the concentration measured molecule and recognition requires two separate successful binding reactions to occur [22]. Thus this type of immunoassay has usually high selectivity, high sensitivity and the lowest LLD. However, after the addition of the sample and each reagent a washing step usually follows, making the assay type laborious a hard to automate. [7]

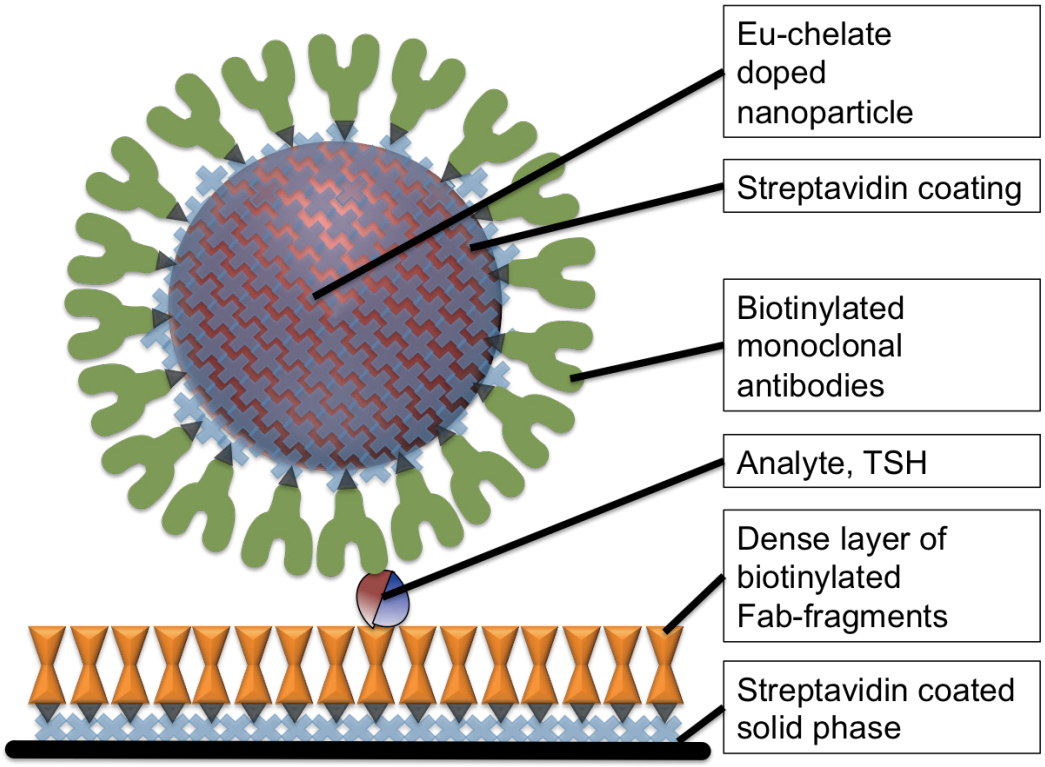

Figure 1. Schema of sandwich-type TSH-immunoassay utilizing a bioconjugate nanoparticle as a label. Optimized configuration contained Mabs on particle surface and site-specifically biotinylated Fab-fragments on solid-phase.

Non-competitive, homogeneous

This immunoassay type relies on signal modulation and direct binding of a detector antibody to a sample molecule. This assay type is easy to execute and automate and commonly used in high throughput screening (HTS) [38]. Most of the assays in this category are FRET-based. [7]

2.1.1. Sensitivity and the lowest limit of detection in immunoassays

Sensitivity of an immunoassay has proven to be an ambiguous concept that can refer to, how small analyte quantities can be detected or to what is the change in the signal as the analyte concentration changes one unit. Therefore, the term most commonly used to describe the lowest concentration still detectable is the lowest limit of detection (LLD) [39]. Considering from a diagnostic perspective a result from an assay can be: a quantitative value, a true positive, a true negative, a false positive, or a false negative. In the first three cases the result the assay correctly diagnoses the patient's condition. The latter two give an erroneous result that lead to misdiagnosis and wrong treatment decisions. In order to provide accurate results the diagnostic test needs to detect a sufficiently low amount of analyte present in the sample. According to the analytical chemistry standard the LLD is classified as the signal that is three standard deviations of the background signal, above the background signal.

$$S_{LLD} = S_{bg} + 3 \times SD_{Sbg}$$

The normally distributed variances are usually small, CV < 10 %, and caused by the method-related aspects e.g. low absolute signal level, imprecision of the assay, the affinity of the binder, specific activity of the label and nonspecific binding of labeled binder (Ekins and Chu 1994). These effects are visible in all samples, but the sample matrix type may increase the variance. Assuming that the variance is normally distributed, this means that at C_{LLD} the test has 1 % false positive rate (α-type error) and the rate of false negative (β-type error) is 50 %. The clinically relevant analyte level cut-off, to classify the patient as either sick or healthy, is usually set higher. The cut-off is method dependent and varies from technology to technology. One of the generally accepted cut-off value is the limit of quantitation (LOQ). That is the signal level set to ten standard deviations of the background signal above the background signal.

$$S_{LOQ} = S_{bg} + 10 \times SD_{Sbg}$$

Setting the cut-off at LOQ would generate a negligible amount of false positives and negatives originating from method-related causes. However, another class of the sample-related false positives and negative are a result of an unwanted interaction with a component in the sample matrix (e.g. human anti-mouse antibodies (HAMA) or other autoantibodies). These sample-related variances are present only in a small fraction of individual, typically clinical, samples and the variance caused by them is high. These problems are generally identified only after the method has been taken into clinical use and samples are obtained from a heterogeneous population.

2.1.2. Affinity of antibodies

Antibody's affinity is the measure with which it binds its epitope i.e. antigen determinant [40]. Bonds forming in the binding reaction are ionic interactions (e.g. attraction of opposite charges of amino acids); hydrogen bonds and hydrophobic interactions (Table 1). Affinity constant defined by the Law of Mass Action as the equilibrium at which association and dissociation happen at the same speed.

$$K_a = \frac{[AbAg]}{[Ab] \times [Ag]}$$

Where K_a is the affinity constant (unit M^{-1}), [Ab-Ag] is the concentration of bound antibody-antigen pair, [Ab] concentration of free antibody and [Ag] concentration of free antigen.
From a more simplified standpoint, the affinity constant is the product of the kinetic rate of bonds being formed i.e. association rate or the on-rate and the kinetic rate of bonds breaking i.e. dissociation rate or the off-rate.

$$K_a = \frac{K_{on}}{K_{off}}$$

This equation separates the speed with which the antibody is able to bind to the antigen and the speed with which the bond dissociates i.e. brakes apart spontaneously. Knowing these two parameters are important parameters to be taken into account in designing immunoassays as they determine the time it will take to run the assay. The valency of the system (e.g. two binding sites in an IgG versus one in Fab-fragment) has an effect to the affinity constant.

On a practical standpoint, it is often easier to measure the dissociation constant K_d (unit M) that is the inverse of affinity constant. The added benefit in this way of defining tightness of binding that it relates the value into the concentration of the antigen in the sample solution. The K_d is the concentration of antigen in moles per liter that is able to occupy half of the available binding sites.

$$K_d = \frac{1}{K_a}$$

Table 1. Equilibrium dissociation constants of certain interaction types [41].

Type of interaction	K_d [M]	Typical examples
Weak	$< 10^{-5}$	Detergent interactions in aqueous micelles
Medium	$10^{-5} – 10^{-7}$	Enzyme-substrate interactions, nonspecific binding of antibodies
Strong	$10^{-7} – 10^{-9}$	Interaction of phospholipids in plasma membrane, protein-protein interactions in signaling, pharmacologically relevant enzyme-inhibitor interactions
Very strong	$10^{-9} – 10^{-11}$	Monoclonal antibody-antigen interaction
Solid immobilization	$> 10^{-11}$	Specific nanoparticle binding, avidin-biotin interaction

2.1.3. Specific activity of the reporter

In order to be detected, antibodies providing the recognition of analyte molecules have to be coupled with a reporter i.e. a label. Signal output from a successful binding reaction is a property of the label. The label here can be e.g. an enzyme, a fluorescent molecule, a radionuclide or a nanoparticle [41]. The higher the signal the easier and more sensitive the detection will be. The very first immunoassays utilized radionuclide reporters such as ^{125}I and ^{32}P, and relied in scintillation counters for detection [1]. The problems with safety and stability of these labels lead to adoption of enzymatic and fluorescence-based detection systems. With enzymatic labels the signal generating reaction progresses until the substrate of the enzyme runs out, and thus integration of signal can be allowed to accumulate, in principle, indefinitely. However, there are shelf life and buffer composition requirements with enzymatic labels that affect their performance and potentially affect assay results [7].

Fluoroimmunoassays (FIA), on the other hand, are inexpensive to carry out, robust and the fluorophores have practically an infinite shelf life (when stored in dry and dark environment) and they produce virtually no spontaneous fluorescence signal. They do suffer to some extent from autofluorescence emitted from plastic ware or biomolecules. Long-lifetime fluorescent reporters, large Stokes'-shift and time-resolved detection were proposed as an optimal strategy in improving sensitivity of fluorescence based immunoassays [42]. The performance of the lanthanide-doped nanoparticles is further enhanced by time-resolved detection of lanthanides. Elimination of short-lifetime background by temporal gating in detection was highlighted as the optimal strategy to improve sensitivity in FIAs [43]. Chelate complexes of

rare earth metals, primarily europium(III) and terbium(III), have a long-lifetime fluorescence emission up to milliseconds, enabling efficient time-resolved detection. [44]

Fluorescent nanoparticles have distinct physical advantages over conventional dye molecules in the solution; they have e.g. an abundance of fluorophores, more surface area available for binders, fluorophores protected from the environment [45] and increased photostability. Dye nanoparticles, dye-doped nanoparticles, semiconductor and metal nanoparticles have all been applied as reporters in bioanalytics [22]. Lanthanide-doped nanoparticles represent one of the most prominent of nanoparticulate fluorescent probe types [18] and [38]. This is due to their excellent physical, chemical and optical properties: availability of multiple lanthanide ions providing different, well-separated emission wavelengths, size and shape-independent luminescent properties, large effective Stokes shifts, long fluorescence lifetime, sharp emission peaks with band-widths of 10 to 20 nm, low photobleaching, exclusion of interfering environmental agents, low toxicity and absence of blinking. These unique properties make lanthanide-doped nanoparticles highly suitable fluorescent probes for applications that need to provide superior sensitivity. [46]

2.1.4. Background signal and noise in FIAs

Over the course of fluorescence based immunoassay development, most of the sensitivity limiting noise-signal produced by light scattering, natural fluorescence of biological samples and other assay materials have been eliminated by careful selection of labels and optimisation of detection instruments [46], [32], [47] and [22]. The autofluorescence is more abundant on shorter wavelengths that possess enough energy to excite the majority of photophysicsally active molecules. Hence, shifting excitation and emission to longer wavelengths over 450 nm reduce the effect of autofluorescence. The scattered light from excitation source, as well as, the autofluorescence, is visible in wavelengths close to the excitation, so selecting a fluorophore-label with a large Stokes'-shift further reduces the effect of autofluorescence signal. The effect of a fluorescence signal emanating from sources other than the label, can virtually be eliminated by applying time-resolved detection of the label, in addition to the two strategies mentioned above [42] and [39].

Specificity of the reaction is another characteristic of the antibody and reflects the antibody's ability to differentiate between epitopes. Some antibodies can differentiate between different enantiomers of the same molecular structure. If an antibody recognizes other epitopes, the interactions are termed as cross-reactivity [48]. These unwanted binding reactions might give rise to false positive results in the immunoassay. This signal is termed as the background signal, since the unwanted binding of the specific label produces it.

2.2. Nanoparticulate labels

In numerous applications sensitivity enhancements exceeding conventional enzyme and radiolabels have been demonstrated in nanoparticle-based labelling systems [49] and [22]. Detection methods based on particulate labels with high specific photoluminescent activity, such as quantum dots [50], luminescent inorganic crystals [51], up-converting phosphors [20], fluorescent nanoparticles [17], [18] and [52], and plasmon resonant particles [19], have been introduced in response to increasing demands in assay sensitivity.

Nanoparicles are defined to have a diameter between 1 to 100 nm and they should exhibit

size-related properties not observed in bulk material. Although, as it may be ambiguous whether a certain property is significantly different from properties of bulk matter, the size-range is de-facto considered to be the defining parameter. However, due to their size nanoparticles act as an intermediate between bulk matter and single molecules and proteins that typically have diameters from 1 to 15 nm [22]. Most of the special characteristics of the nanoparticles derive themselves from the fact that in nanopartcles the amount of surface-atoms compared to total amount atoms i.e. nanoparticles have a high surface-area-to-volume – ratio (AV-ratio). The surface atoms carry also another functionality, they serve as a protective layer for the fluorophores that prevents destructive photobleaching, eliminates dynamic quenching and stabilizes the microenvironment to eliminate solvent relaxation of excited fluorophores [45]

In some materials e.g. semiconductors and gold the size of the nanoparticle determines the optical properties of the colloid. In semiconductor nanoparticles the small size of the particle allows quantum confinement of energy states and thus the free movement of electrons in the lattice is obstructed. Furthermore, the colloids absorb photons that excite electrons to higher energy states and in the relaxation process a lower energy photon is emitted. Semiconductor nanoparticles absorb light mainly in the UV/Vis(blue) – wavelengths, but also red and near-IR [53] and [54]. They emit a narrow peak corresponding their size or more accurately band gap between the highest valence band and the lowest conduction band. Colloidal gold (3-100 nm) absorbs light according to its size, but whereas it does not emit light it can form surface plasmons. However, as a prime example of size dependent properties of nanoscale materials, the ultra-small gold nanoclusters, size < 1 nm, are again fluorescent, water soluble and good labels for *in vitro* -diagnostics [55] and [56].

The primary motivation for utilization of nanoparticles in immunoassays is that they can provide higher specific signals per binding reaction than molecular dyes and most enzymes [57] and [58]. The specific activity of a label is determined by how much signal it produces when compared to the background. Fluorescence and phosphorescence emission are both very specific reactions and in an optimized detection setting there is virtually no spontaneous background emission or reflection. Hence, the background signal is usually very low compared to, for example absorbance. The specific activity of nanoparticles is readily modifiable as the size of the colloid or the dye molecules incorporated within the particle can be chosen to accommodate the needs of any application. However, many fluorophores exhibit self-quenching when they are packed inside of the nanoparticle core, well within the Förster-radius of the fluorophores. In this respect, the lanthanide-doped nanoparticles stand out as they have an extremely long Stokes-shift, originating from the complex photophysical relaxation of the excited state [42].

Besides the size and labeling other key determinants of a nanoparticle label are surface charge, hydrophobicity/hydrophilicity and biofunctionalization. A strong surface charge, either negative or positive, is required to achieve and maintain particle-particle repulsion that will disallow the aggregation of nanoparticles. In diagnostic applications, the particles are usually designed to be as hydrophilic as possible. Anti-fouling agents are mainly hydrophilic polymers e.g. polyethylene glycol or proteins e.g. BSA [25].

2.2.1. Bioconjugate nanoparticles

To be utilized in immunoassays the nanoparticles need to be coated with antibodies. To

achieve this there are various technologies ranging from nonspecific physical adsorption, elaborate bioconjugate chemistry to site-specific bioconjugation of antibody fragments and over to use of adaptor proteins, e.g. avidins (Table 2), as reviewed by [47]). The method of bioconjugation affects the density of coating, orientation of biomolecules and the stability of biomolecules. All of the parameters listed have further implications for the binding properties of bioconjugate nanoparticles.

Table 2. Summary of bioconjugate chemistry functionalization reactions typically utilized with nanoparticulate labels, adapted from [47]

Target	Reactive Group	Product	Example mecanism
Free thiol -SH	Maleimide	Thioether	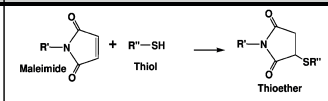
	Haloacetyl or Alkyl halide	Thioether	
	Arylating agents	Thioether	
	Aziridine	Thioether	
	Acryloyl derivatives	Thioether	
	Disulfide exchange - pyrfyridyl disulfides, 5-thio-2-nitrobezoic acid (TNB)	Mixed disulfides	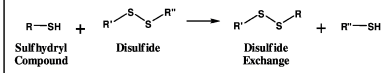
Aldehyde or Ketone -CHO	Hydrazine	Hydrazone	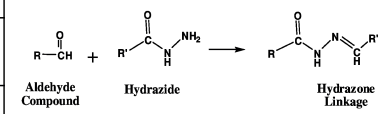
	Amines	Schiff's base (imine)	
Free amine -NH_2	*N*-hydroxysuccinimide ester (NHS)	Amide	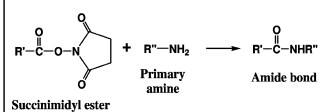
	Acetyl azides	Amide	
	Isocyanates, Isothiocyanates	Urea, Thiourea	
	Sulfonyl chlorides	Sulfonamide	
	Aldehydes, Glioxals	Imine, Secondary amine	
	Epoxides, Oxiranes	Secondary amine	
	Carbonates	Carbamate	
	Arylating agents	Arylamine	
	Imidoesters	Amidine	
	Carbodiimines, anhydrides	Amine	
Carboxylate	Carbodiimines	Amides	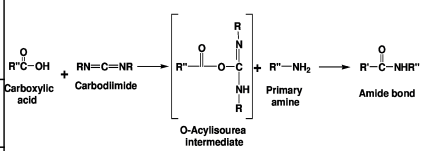
	Carbonyldiimidazole	Amides	
	Diazoalkenes, Diazoacetyl	Ester	
Hydroxyl	Epoxides, Alkyl halogens	Ether	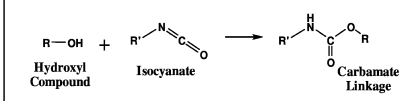
	Periodate	Aldehyde	
	Carbonyldiimidazole	Carbamate	
	Isocyanates, Isothiocyanates	or	
	N-hydroxysuccinimidyl chloroformate	Urethane	
	N,N' -disuccinimidyl carbonate		
Ractive carbon (e.g. phenol on tyrosine)	Diazonium	Diazo-bond	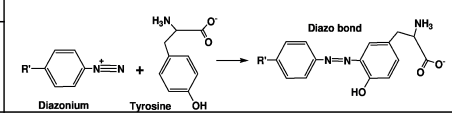

Polystyrene is weakly hydrophobic and that facilitates physical adsorption to surfaces as a bioconjugation method. Also, the native conformation of a protein is determined by folding of the hydrophobic residues that allow close packing of protein cores [59]. The effect of the surface chemistry of biomaterials on the protein adsorption process has been a topic of great interest for many years, and much is known in this field [60]. Interaction with a surface can easily disrupt the native conformation and, therefore, the protein function. This renders a number of the conjugated antibodies unable to bind intended targets. In addition effects caused by denaturation, the orientation of binding sites is random and not all of them can access the antigen. A classic example of bioreactive adaptor protein using coupling is the biotin-streptavidin system, which can be classified as nearly covalent by its affinity with a K_d 1×10^{-14} M [61].

Avidity of a labeling unit – nanoparticle coated with multiple antibodies – has been shown to

exceed that of the soluble labeled antibody. The probability for successful binding has increased together with multiple binding sites. Increase in the association rate constant contributes favorably to the improved affinity and more than ten-fold higher affinity constants have been measured for nanoparticle bioconjugates [23]. High specific activity and high avidity have made possible to decrease the number of detector antibodies in immunoassays.

2.2.2. Colloidal stability

One of the main characteristics of nanoparticles in suspension is that the nanoparticles are properly dispersed i.e. they form stable colloids. Nanoparticle suspensions are stabilized by the high surface charge of the particle and by agents in the suspension that enhance electrostatic or steric stability [62]. Stabilization is required to counteract the Van der Waals attraction forces that would otherwise cause the particles to aggregate and sediment. The parameter used to measure electrostatic stability is zeta potential (ζ -potential) [63]. It can be defined as electrophoretic mobility of the colloid and it is a measure of the electrostatic repulsion force between charged particles. The higher the absolute value, positive or negative, is the stronger repulsion is and the more stabile the suspension is. The particle is surrounded by a double layer (DL) of ions with an inner dense shell of ions, called the Stern layer, with an opposite charge to the surface charge and an outer, more diffuse, layer of ions with a matching charge (Figure 2). Physiological environment the surface charge is thus not in direct contact with the surrounding buffer and surfaces, but the effect of the charge dissipates through these layers. Hence, in case of nanoparticles, the surface potential and the Stern-potential are usually much higher than the ζ -potential. Ionic strength of the solution is inversely proportional to the Debye length that is the width of the DL in physiological ionic strength of 150 mM is around 1 nm and in e.g. 1 mM it would be 10 nm [63].

However, in the case of bioconjugate nanoparticles the surface charge alone does not define the stability of the colloid (Figure 2). The antibody layer covering the nanoparticle reaches much further than DL of ions. The bioconjugation strategy, usage of adaptor proteins, the stability of coated antibodies and the size of the antibody type will all be effective parameters in determining the colloidal stability. Furthermore, to the antibody surface is adhered a loosely bound corona of proteins in the assay matrix or assay buffer. The addition of nonpolar surfactants or polymers enhances stability through steric stabilization of the bioconjugate nanoparticle's surface.

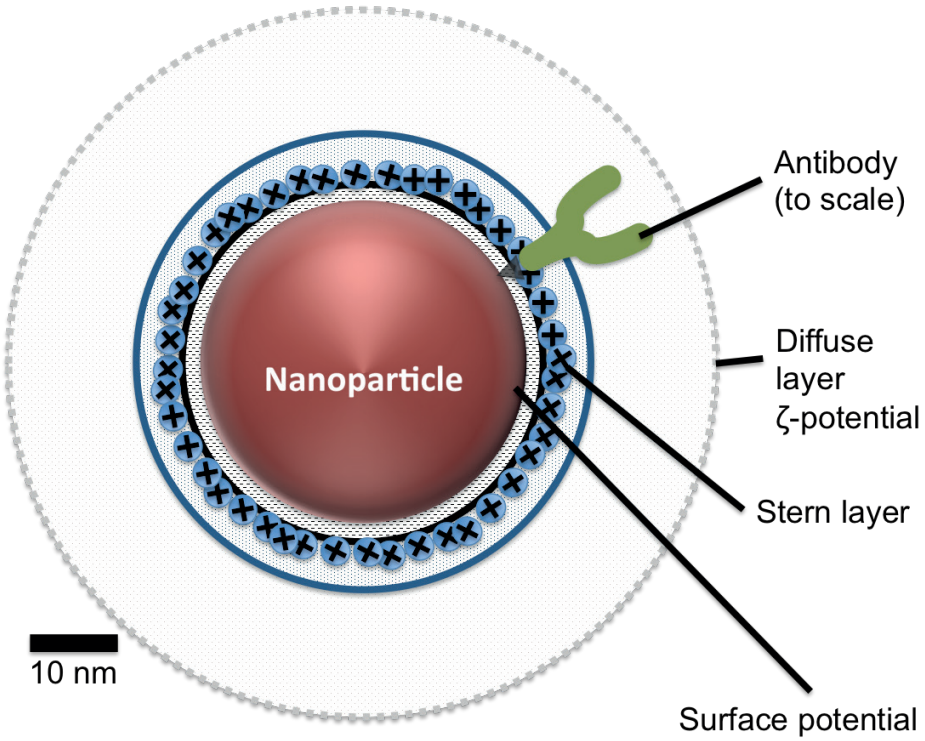

Figure 2. Charged layers on a nanoparticle biconjugate.

2.2.3. Kinetics of nanoparticle binding

The high AV-ratio and the high number of binding sites of biofunctionalized polystyrene nanoparticles contribute to stronger binding of nanoparticles when compared to labeled single molecules [64]. Previous research supports approximately ten-fold increase in overall affinity, K_d, demonstrating that increased avidity and slower dissociation more than compensate the slower diffusion. Furthermore, due to the close proximity of adjacent binders and nonspecific binding of the particle the dissociation is slower [65] and [23]. These properties both increase the affinity of the label, i.e. they make binding more probable and stronger. However, these phenomena are equally observed for nonspecific binding limiting the applicability of nanoparticle labels [66].

The dissociation constant of the specific binding of bioconjugate nanoparticle to PSA attached to solid-phase antibodies was measured to be 1.8×10^{-11} M compared to the 1.5×10^{-10} M given by the provider for single Mab [23]. The kinetic constants were calculated by running a global fit of a concentration series [67]. The association rate (constant), k_{on},of specific binding was measured to be 2.5×10^{6} M^{-1} s^{-1} and the dissociation rate (constant), k_{off}, was determined to be 3.7×10^{-5} s^{-1} [23]. However, the k_{off} was so low that the dissociation could be considered too slow to be measured and also the standard error for k_{off} parameter was very high. The result in line with previous observations that the lifetimes of typical protein–protein complexes range from microseconds to weeks, and protein–ligand complexes typically have lifetimes of microseconds to days. The association rate constants of some complexes approach the diffusion-controlled limit, whereas conformational changes upon binding may slow down the

process by orders of magnitude [68].

2.3. Solid-phases in sandwich-type immunoassays

Creating binding surfaces with high specific binding activity and low nonspecific binding is a prerequisite for a high sensitivity bioaffinity assay. The most common solid surface of choice has been polystyrene as it is easily molded and has a good ability to adsorb proteins. Relatively strong hydrophobic bonds are formed upon adsorption between the hydrophobic amino acids and the polystyrene monomers [69]. Different methods, irradiation, plasma-treatment etc., are available to modify surface characteristics altering the profile of adsorbed proteins from hydrophobic to hydrophilic [70]. In most cases, the capture protein layer is not complete and there is a need for blocking the surface with additional proteins or detergents [69] and [71]. Blocking molecules are usually chosen to readily adsorb onto the polystyrene surface and have no affinity towards binding molecules in order to prevent their nonspecific binding.

Passively adsorbed proteins on any given surface alter the conformation of these proteins [72]. In case of polystyrene and silicone there is evidence that proteins unfold permitting internal hydrophobic side chains to form strong hydrophobic bonds with the surface [69]. While the bond between surface and proteins is strong and relatively stable, the altered conformation has been proven to affect antigen specificity and function. Also, the protein surface adsorption has been reported to denature a large portion of adsorbed antibodies and significantly reduce the amount of binding sites [69] and to change enzyme substrate specificity [73] and [74]. It has been shown that the method for attaching capture antibodies has an impact on the functionality of the antibody layer [75] and [27]. In the case of the scFv-fragments lacking the stabilizing constant domains it has been suggested that the partial unfolding of the antibody fragments creates sticky patches on the surface leading to increased nonspecific signal [76]. It has previously been shown that both, whole monoclonal antibodies and their fragments, have improved performance in and immunoassay, when they are attached to microtiter well surfaces via capture proteins [30] and [40]. However, no change in respect to nonspecific binding was found when fragmented antibodies were applied in the nanoparticle assays. [34]

The edge effect has been identified as potential mediator of increased adsorption of material evidence of sites that are prone to nonspecific binding [77] and [75]. The topographic features on coated surfaces, both increase the surface area increasing the binding capacity and cause turbulent liquid flows that hasten the binding kinetics [78]. However, the unwanted increase of the microtiter well edges and other topographical features on nonspecific binding of labeled molecules has been reported [79]. The large surface area in the edges could potentially lead to higher degree of nonspecific binding of nanoparticles compared to flat surface areas containing no edges [77].

2.4. Nonspecific binding in bioaffinity assays

Unwanted nonspecific binding of the labeled detector antibody is a universal problem in immunoassays and bioaffinity assays in general. It is acknowledged as one of the main limiting factors in further improvement of sensitivity in bioaffinity assays utilizing bioconjugate nanoparticle [51] and [80]. The origin of the phenomenon has been widely speculated, but it has not been clearly characterized due to its diverse nature. However, it can

be divided into two categories, in terms of sample-to-sample variation, constant and variable.

There are at least three possible reasons for constant nonspecific binding: 1) the surface itself adsorbs the label (labeled antibody) or 2) the capture protein attached to the capture surface binds the label or the antibody attached to it or 3) the surface structure of the solid phase promotes nonspecific binding. Generally, this kind of nonspecific binding is a sum of a wide variety of interference [48]. In non-clinical setting buffer matrix, the nonspecific binding of bioconjugate nanoparticles has been shown to depend on the amount of antibodies on the particle surface [81]. This can be circumvented in some degree by variety of coating procedures, buffers and optimization of the assay [82].

The variable nonspecific binding is likely to be caused by the sample matrix e.g. human anti-mouse antibodies, rheumatoid factors, complement reaction, heterophilic antibodies or autoantibodies in blood or serum [48] and [83]. In such cases, the term false positive is often used, implying differences between samples and a majority of these cases are caused by specific cross-reactivity of one or more components of the assay. The Fc-part, responsible for mediating the immunoregulatory functions of antibodies, has been linked to some of the interfering effects and utilization of fragmented antibodies has in some cases reduced the occurrence of variable-type nonspecific binding [84] and [85]. Adding an excess of structurally similar, nonspecific bovine or murine immunoglobulin or other proteins to the assay buffer to deplete the origin of cross-reactivity has been shown to reduce the problem, but not to eliminate it [81] and [86]

2.4.1. Bond types in nonspecific binding

Intermolecular interactions in nonspecific binding are comprised of similar interactions as specific binding, but from an assay development standpoint, these binding events are unwanted. The hydrophobic interactions, specific chemical interactions, hydrogen bonding, and the electrostatic interactions between proteins and the adsorbent mediate bond formation. In addition to general adsorption, cross-reactivity, antibody interference and matrix effects are included in nonspecific binding. When nanoparticles enter a biological fluid, they become coated with proteins that may transmit biological effects due to altered protein conformation, exposure of novel epitopes, perturbed function (due to structural effects or local high concentration), and/or avidity effects arising from the close spatial repetition of the same protein [68].

2.5. Antibody fragmentation to reduce nonspecific binding

Majority of the immunoassays and clinical applications that are commercially available make use of whole Mabs [40]. The offer stability and proven functionality developed over millions of years of evolution. However, Mabs are meant to transmit the recognition signal on to immune cells and for this purpose they have functionalities also in the Fc-domain. These functionalities, on the perspective of immunoassay development, tend to cause unwanted interferences in the assays [87]. Recombinant DNA technologies have facilitated the fragmentation of antibodies into single-chain variable-Fv (scFv) or Fab fragments containing the domains required for antigen recognition, but lacking the Fc-part (Figure 3) [88], [40]. Owing to their smaller size and the lack of parts not involved in antigen recognition, the recombinant antibodies can provide advantages in immunoassays. The effect of different antibody fragments (scFv or Fab) on immunoassay performance has been studied with

surface plasmon resonance [89]. The Fab fragment was found to be more resistant to variations in assay configuration compared to scFv fragment. In another study, two monoclonal antibodies have been compared to recombinant Fab fragments in sandwich-type time-resolved fluorescence immunoassay for cardiac troponin-I [29]. The authors found that recombinant Fab fragments improved binding capacity, yielded many fold higher signal levels and increased assay sensitivity. Yet another study compared three different antibody formats (Mab, Fab and scFv) in sandwich-type immunoassay of TSH [34]. Mab, Fab and scFv were used as capture antibodies and detector antibody was directly labeled. The background signal was reported to be two-fold higher with scFv fragments compared to Mabs and Fab fragments.

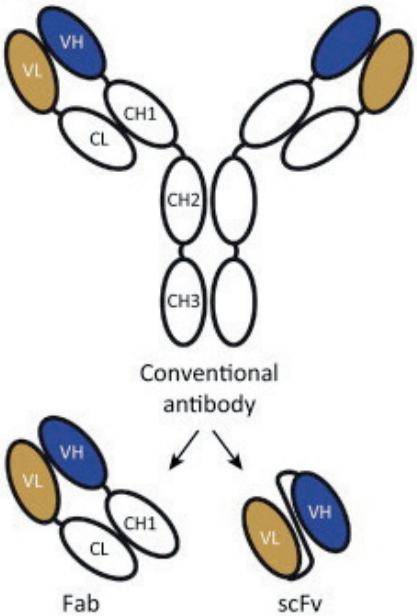

Figure 3. A Schematic representation of a whole monoclonal antibody (Mab), Fab-fragment and scFv-fragment, adapted from [88]

2.6. Matrix related problems in immunoassays

Matrix effects in an immunoassay usually refer to interference arising from the sample matrix (e.g. whole blood, serum or saliva) that contains the analyte, but in a broader sense it means all the other components, including assay buffer, plastic ware, separation system and cross-reactivity of antibodies [90]. It is defined to be variation in the reactivity of the analyte caused by variations in its environment in the sample that includes properties like pH, ionic strength, different proteins and lipids with varying concentrations, cross-reactivity with sample components and antibody interference (e.g. human anti-mouse antibodies). In most of the diagnostic immunoassays blood or a fractionated component of it is the sample matrix [91]. Matrix effects cause variations in the reactivity of the analyte towards other components in the assay or secondary reactions that affect the binding of the labeled antibodies, and due to these variations the result of the assay no longer reflects the true concentration of the analyte in the sample [90]. [7]

The whole blood may be used in some immunoassays, especially in neonatal screening for congenital defects, because sample volume is very limited and does not allow pre-analytical

processing. The presence of chromogens and enzymes which include proteases, hydrolases and those capable of generating active oxygen species such as superoxide dismutase, peroxidases and pseudoperoxidases (haem nucleus) can lead to nonspecific effects, especially in non-optimized enzyme immunoassays based on peroxidase reaction products as a signal. The proteins in plasma [92] and serum [93], the presence of complement [94], rheumatoid factor [95], chelators [96], polyanions [97], autoantibodies [98], other cross reacting antibodies [99], drugs [100] and metabolites of the analyte in question may give rise to nonspecific effects which may be specific only for one specific assay system in question or all employing a certain reagent. In serum the same problems can occur, with the exception of the anticoagulants, fibrinogen and clotting factors. The fact that the lowest frequency of interference effects due to the sample matrix is seen in assays using serum as the sample may reflect the fact that the majority of assays have been "optimised" with respect to serum as the sample matrix. [101]

Mechanisms through which interfering compounds affect

Types of interference in immunoassays include: 1) cross-reactivity; 2) the hook effect; 3) antibody interference; 4) signal interference; and 5) matrix related effects. Some immunoassay designs are especially prone to particular types of interference e.g. competitive immunoassays are susceptible to the hook effect, whereas non-competitive are not.
Immunoassays are often quite sensitive to the matrix due to effects on antigen antibody binding, efficiency of separation of bound and unbound fractions, and the extent of nonspecific binding.

Interfering, endogenous substances that are natural, polyreactive antibodies or autoantibodies (heterophiles), or human anti-animal antibodies together with other unsuspected binding proteins that are unique to the individual (Table 3), can interfere with the reaction between analyte and reagent antibodies in immunoassay [87].

Table 3. Interferences are very case-specific, hard to predict and difficult to detect. They may increase or decrease the measured value and result to misdiagnosis and to insufficient or dangerous clinical decisions.

Unique to an individual
Interfering antibody concentration can change over time within the same individual
Low affinity polyspecific antibodies can be present in high concentrations or high affinity in low concentrations
Can produce falsely high (false-positive) or falsely low (false-negative) results
May interfere within one or more manufacturers' immunoassay systems but not necessarily in all assays
May interfere in a number of immunoassays for different analytes
The inclusion of one or more interference blocking agents in manufacturers' immunoassay reagents may be insufficient to overcome the interference

A list of methods used to reduce interference caused by heterophile antibodies and HAMA (Table 4), [90], [48] and [87].

Table 4. The procedures through which immunoassay interference can be removed. There are two principle strategies; removal of the interfering compound or rendering it non-functional.

Removal of interfering antibody	Prior extraction of analyte from sample, e.g., by chromatography		
	Immunoextraction	Murine or other animal species serum immobilized onto microbeads	Immobilized Protein A tubes or beads
	Polyethylene glycol precipitation (PEG 6000)		
	Heating to 70–90°C (for heat-stable analytes only)		
Addition of blocking agent from the same species as the antibody reagents	Non-immune serum, species-specific polyclonal IgG, anti-human IgG or polymerized mouse IgG		
	Non-immune or denatured mouse monoclonal antibodies		
	Species-specific fragments of IgG [Fc, Fab, $F(ab')_2$]		
	Heterophile blocking reagents, immunoglobulin inhibiting reagent, and anti-assay antibody blocking tubes		

Affinity purification

In study that reported an interference caused by HABs, Preissner et al. re-assayed several months of stored samples after HBT treatment. In another group of an additional 1751 samples they found a similar heterophile interference rate of just fewer than 2.9%. They suggest to routinely treating all samples in heterophile blocking tubes HBT tubes before serum thyroglobulin measurement. This has brought the heterophile interference rate down to excellent, and in this case known and verified, levels of less than 0.1% [91]. This is reflected by the fact that depending on the assay used, the published estimation of the HAMA prevalence in the normal population varies between 1–80% [91] and many studies show that the prevalence of interfering antibodies affects 30-40% of the population [48]. Consequently, these assays have limited value in excluding or confirming any suspected clinically relevant HAB interference.

2.6.1. The protein corona of bound biomolecules

As much as the nanoparticle material and the bioconjugate layer, the nanoparticles can be classified in terms of their biomolecule corona [102]. The biomolecule corona of a nanoparticle is a dynamic layer of non-covalently associated proteins and other biomolecules that in part, mediates nanoparticle interactions and biological identity of the bioconjugate nanoparticle [102]. Protein adsorption to various materials has been widely studied and it has been found that various factors *e.g.* electrostatic interactions, hydrophobic interactions, and the specific chemical interactions between the protein and the adsorbent mediate bond

formation. The effect of the surface chemistry of biomaterials and their effect on the protein adsorption process has been studied in detail [60] and [69]. Selective adsorption of proteins on various synthetic adsorbents has been examined under different conditions (such as solution pH and protein concentration) and for many proteins the mechanism of selective adsorption has been attributed to electrostatic interactions [103]. Anti-fouling strategies in medical device research, such as PEGylation of the surface, are utilized to minimize protein deposition [104]. The interactions are complex, and a reduced protein load on the interface does not necessarily mean a reduced amount of interactions as compared to adsorbed protein.

The native conformation of a protein is tightly controlled by the shape complementarity of the hydrophobic residues that allow close packing of the cores[59]. Interaction with a surface can disrupt the native conformation and thus modify protein interactions and its function. Proteins such as fibrinogen, lysozyme, ovalbumin, and human carbonic anhydrase II) bind with no enthalpy change. Thus, the binding of these proteins is likely to be driven by an entropy increase as bound water is released from the surface of the nanoparticle. This more than compensates the reduction of entropy of the protein. In the case of entropy-driven binding, the initial interaction does not result in a conformation change of the protein, however, a secondary reaction driven by electrostatic interactions is possible after an initial interaction [105]. At the interface between asbestos fibers and the biological medium, homomolecular exchange between the adsorbed and dissolved state of BSA was studied with Fourier transform infrared spectroscopy (FTIR) and CD spectroscopy. In the solid state, BSA modifications were driven by surface interaction with the substrate and once BSA is desorbed back into the solution its structure rearranges, although some of the modifications with respect to the native species are irreversible [106]. Same observations have been made with polystyrene nanoparticles, the adsorption and subsequent desorption of BSA from polystyrene particles causes irreversible changes in its stability, secondary and tertiary structure [107]. This, in turn, can lead to myriad of secondary interactions of the denatured proteins.

3. AIMS OF THE STUDY

I. Characterize nonspecific binding in immunoassays utilizing nanoparticle labels

II. Study mechanisms that induce nonspecific binding

III. Measure the difference in bond strength between specific and nonspecific binding immunoassays utilizing nanoparticle labels

IV. Measure the parameter best able to differentiate between specific and nonspecific binding

V. Develop methods to reduce nonspecific binding in immunoassays utilizing nanoparticle labels

By using nanoparticle labels a superior intensity of the produced signal can be obtained, as in essence a single binding event can be visualized [5]. The antibody-coated nanoparticles have higher binding avidity than single antibodies [23]. However, the major disadvantage of the nanoparticle labels is the increased background signal resulting from nonspecific binding of the antibody-coated nanoparticles. The study was undertaken to solve original causes of this sensitivity-limiting problem and to find ways to reduce it, in order to improve the LLD and sensitivity of sandwich-type immunoassays.

The first aim was to do a thorough step-by-step characterization of the impact of the different components of the assay setup have on the nonspecific binding. We studied the effects of particle size, antibody fragmentation, solid-phase coating and nanoparticle bioconjugation strategies. Here we found certain factors that correlated between assays for PSA and TSH e.g. optimal antibody configuration, colloidal stability of bioconjugate nanoparticles and binding kinetics of nanoparticles, thus these parameters are likely to be general guidelines in designing immunoassays utilizing nanoparticle labels. As the second objective, these phenomena were examined and the parameters contributing the most to the nonspecific binding were revealed. The third objective was to measure the relative bond strengths of specific and nonspecific binding. To our surprise the bond strengths were very close to each other and as such the most obvious parameter to differentiate between specific and nonspecific binding was unusable in the development of more sensitive immunoassays. This finding, in turn, lead us to the fourth objective that was to find and measure the parameter that is the reason behind the vast difference in biding observed with analyte present as compared to the absence of the analyte. The final, and the most important objective, was to make use of this new information in developing a more sensitive immunoassay utilizing nanoparticle labels.

4. SUMMARY OF MATERIALS AND METHODS

4.1. Nanoparticle bioconjugate chemistry

The nanoparticle type utilized in all of Publications **I**, **II**, **III** and **IV** was europium(III)-chelate (β-diketone) – doped Fluoro-MaxTM, monodisperse, carboxyl group – functionalized, polystyrene nanoparticles (101, 53.5, 46 34 and 23.5 nm in radius) that were purchased from Seradyn (Indianapolis, IN). The particles contained 2.94, 1.77, 2.78, 0.96 and 1.11 carboxyl groups per nm^2, respectively; these were used for covalent bioconjugation. The number of europium(III) ions in a single nanoparticle was determined by adding the nanoparticles to a 1 mL/L Triton X-100 solution or to the enhancement solution (DELFIA; Perkin-Elmer Life Sciences).

For the antibody type experiments [**I**] nanoparticles were prewashed with 10 mM phosphate buffer, pH 7.5, on a Nanosep microporous centrifugal filter (300 kDa cutoff; Pall Filtron). Phosphate buffer was added to the particles, and the solution was sonicated with a tip sonicator (Labsonic U; B. Braun) at 80 W for 5 s. Carboxyl groups on the surface of nanoparticles were activated with 10 mM *N*-(3-dimethylaminopropyl)-*N*′-ethylcarbodiimide and *N*-hydroxysulfosuccinimide (Fluka) for 30 min. The activated particles were washed once with 10 mM carbonate buffer, pH 9.0, and 15 μM streptavidin was added. After 2 h of incubation, the streptavidin-coated particles were washed five times with a 2 mM Tris-HCl solution, pH 7.4, and stored at 4 °C.

Alternatively, the Mab anti-TSH 5404 [**II**], [**III**] and [**IV**] was covalently coated to nanoparticles according to above-described procedure using 6 μM mAb [108]. The monoclonal antibodies were botinylated randomly through lysines according to protocol described earlier [34].

4.2. Well-plate immunoassays

4.2.1. Nanoparticle and sample preparation

To produce bioconjugate nanoparticles [**I**], biotinylated antibodies were attached onto the SA-coated nanoparticles in the assay buffer for 60 minutes. The nanoparticle bioconjugates were then sonicated with a bath sonicator, vortexed vigorously and 2 mM biotin was added to block the remaining SA and the incubation was continued for another 5 minutes. When the covalently coated MAb anti-TSH 5404 bioconjugate nanoparticles were used this step was omitted [**II**], [**III**] and [**IV**].

Affinity purification

Affinity purification performed by incubating pooled human serum in microtitre wells coated with anti-TSH Mab 5404 (**IV**). Alternatively, the serum was purified with anti-PSA Fab 5A10 that was structurally similar to the anti-TSH antibodies. The incubation lasted 15 minutes and the serum was treated twice in a volume of 60 μl. The purified serum was extracted from wells and stored refrigerated or frozen until used. The purified serum diluted 1-20 fold into KVG-buffer immediately prior to measurement.

4.2.2. Well-plate sandwich-type immunoassay

In all publications streptavidin-coated microtitration wells were washed twice with the wash solution to remove preservatives and loosely bound proteins. In the first step 3×10^{-13} mol or 2×10^{11} molecules of the biotinylated capture antibodies were attached to the solid-phase in 30 µl of assay buffer for 20 minutes. To create the spot-wells (**IV**) streptavidin-coated microtitration wells were first washed twice with the washing solution to remove preservatives and loosely bound proteins. In the second step 3×10^{-13} mol of biotinylated Fab-fragment were incubated in 30 µl of KVG-buffer for 20 minutes. In spot-coating 1×10^{-13} mol of biotinylated Fab-fragment was incubated in volume of 1 µl of KVG-buffer for 10 minutes. The spot was produced by adding the 1 µl drop of capture-antibody halfway between the edge and center of the well of a streptavidin functionalized 96-well plate. The majority of the solid phase is left devoid of the capture-antibody and affinity of the bioconjugate nanoparticle towards it is significantly lower.

In all publications wells were washed to remove unbound antibodies. Thereafter, analyte, 1.5×10^{9} molecules of prostate specific antigen (PSA, 2×10^{-6} g/l or 75×10^{-12} M) or TSH (10 mIU/l or 66×10^{-12} M), was added in 35 µl of assay buffer and incubated for 20 minutes. After the reaction, the wells were washed twice to remove unbound analyte. Then 3×10^{7} - 1×10^{9} nanoparticle bioconjugates (depending on the assay format) were added to wells in 40 µl of assay buffer and incubated for 30 or 120 minutes. In the study for nanoparticle size, incubation times of 120, 240, 480 and 1140 with three replicates were used. Finally, the wells were washed six times, and the surface-bound europium fluorescence from the nanoparticle–antibody bioconjugates was detected at 615 nm using a time-resolved plate fluorometer Victor^2 1420 Multilabel counter (Wallac, PerkinElmer Life Sciences). Immunoassay with SA-Eu [**I**] was performed as described for immunoassay with nanoparticles by replacing the nanoparticle bioconjugates with 3×10^{11} (500 fM) SA-Eu molecules and using 30 minutes incubation for the bioconjugate.

4.2.3. Optimized sandwich-type immunoassay with serum samples

To stabilize the protein corona the bioconjugate nanoparticles the particles were diluted 5-1000 fold into KVG-buffer or to a subset of buffer's components (**IV**). Thereafter, the desired amount analyte, thyroid stimulating hormone (TSH), was added KVG-buffer and incubated for 20 minutes. Alternatively, the TSH was mixed into affinity purified serum – KVG-buffer – mixture and incubated 10-20 minutes. In the one-step assay configuration TSH was added into 1:1 mixture of affinity purified serum and KVG-buffer and 20 µl of the sample was then added to the reaction well. After 10 minutes the detector bioconjugate nanoparticles 3×10^{7} in 30 µl of KVG-buffer were added to wells and incubated for 30 minutes. Finally, the wells were washed six times, and the time-resolved fluorescence from the nanoparticle–antibody bioconjugates was measured at 615 nm using tme-resolved fluorescence of plate reader Victor^2 1420 Multilabel counter (Wallac).

The LLD was calculated (**I** and **IV**) by first subtracting average background signal from the calibrator sample averages. The standard deviation of the background replicates (N=5) was calculated. After that we fit a power-function to the background subtracted signal values.

$$y = ax^b$$

From parameters of this equation the LLD was set to 3×SD.

$$LLD = (\frac{3\times SD}{a})^{\frac{1}{b}}$$

4.2.4. Stability of antibodies

The solid-phase antibody Mab anti-TSH 5409 was immobilized on clear MaxiSorp™ microtitration wells by physical adsorption [**II**]. The wells were coated for overnight at 37 °C with 100 ng of Mabs in 50 µl of 10 mM phosphate buffer, pH 7.0. The coated wells were washed twice with a wash solution and saturated over night at 23 °C with 200 µl of 10 mM phosphate buffer (pH 7.0) containing 76 µM bovine serum albumin and 27 mM D-sorbitol. After the saturation, the wells were aspirated and dried in a laminar hood for 1 h. The wells were stored at 4 °C in a sealed package with desiccant.

In publication **II** prior to use, the wells with passively adsorbed Mabs were prewashed four times to remove preservatives. When Fab-fragments or biotinylated Mabs were used the optimized amount (**I**, Figure S1) was added at this stage. As an additional step to the standard protocol, this was followed by denaturing treatments in a volume of 50 µl in case of acids and detergents and 100 µl when heating was applied. A washing step was performed to remove denaturing solution before the continuation of the assay. Thereafter the assay according to the above-mentioned protocol, the analyte, TSH (1 mIU/l), was added in 35 µl of assay buffer and incubated for 20 minutes.

4.3. Antibody fragment production

Cloning of anti-PSA hybridoma cell lines H117 and 5A10 antibodies have been previously described [83] as well as cloning, expression and site-specific biotinylation of anti-TSH antibody clones 5404 and 5409 producing cell lines [34]. All fragments contained an additional unpaired cysteine and his_6–tag peptide at C-terminus of Fd chain (**I**, **II** and **IV**). Fab-fragments were expressed to periplasmic space of *Escherichia coli* strain RV308 (ATCC# 31608) in a 5-L BioFlo3000 fermentor (New Brunswick Scientific, New Jersey, USA) using a high-cell density cultivation technique and the defined medium in 32-36 h time span. Cells containing antibody fragments were collected and stored frozen at -70 °C until purification. Antibody fragments were purified using osmotic shock, Streamline SP (1.2 l in Streamline100 column) expanded bed adsorption chromatography, and finally with 50 ml of a nickel-loaded chelating Sepharose fast-flow affinity chromatography matrix (all from Amersham Biosciences, Uppsala, Sweden). Unpaired cysteine was site-specifically biotinylated with Maleimide PEO_2-Biotin (Pierce, USA). The Mabs were randomly botinylated through lysines according to protocol described earlier [34].

4.4. Atomic force microscopy

AFM-images were captured using NTEGRA Prima scanning probe microscope (NT-MDT, Russia) (Publication II). Surface topography was measured with intermittent contact mode under ambient conditions (T =24–25 °C, RH = 17–34 %) using uncoated rectangular silicon cantilevers (MikroMasch, model NSC14/NoAl or NSC15/NoAl). Images were recorded in the repulsive regime using a damping ratio of 0.7 and a scan speed of 0.25–0.50 Hz. The images were processed with scanning probe image processor (Image Metrology) software. NTEGRA

Prima was also utilized to measure spring constants of MCLT probes (**III**).

In AFM studies, the well edges were removed to make the sample accessible to AFM. In addition, in all experiments measured with AFM, we used 1×10^9 nanoparticle bioconjugates in 15 µl of the assay buffer in order to promote nonspecific binding. Finally, the wells were washed six times, and the time-resolved fluorescence from the nanoparticle–antibody bioconjugates was measured at 615 nm using the plate fluorometer [**II**].

4.5. Force spectroscopy

Force measurements in publication **III**, using AFM tips functionalized with anti-TSH5404-BSA–coated nanoparticles, were performed on surface bound anti-TSH5409 antibodies in the absence and presence of TSH (30 mIU/l) on an AFM 5500 (Agilent Technologies, USA) setup. When distributed evenly on the solid phase, the TSH amount corresponds to 400 TSH molecules per μm^2. To record one PDF, 1000 force-distance cycles were recorded. PDFs were recorded at vertical scan rates ranging from 0.5 to 5 s and *z*-amplitudes from 300 to 1000 nm. In order to vary the contact time of the probe and solid-phase the deflection set point value was changed. This method changes also the indentation force of the tip, but force-distance curves were analyzed only from probes where the nanoparticle was not trapped between tip and the solid phase. The curves where the nanoparticle was trapped, i.e., where the deflection signal in the approach curve showed a decrease after an initial increase or a clearly nonlinear increase, were excluded. All measurements were performed in assay buffer (10 mM NaH_2PO_4 (pH 7.4), 150 mM NaCl, 7.7 mM NaN_3 and 75 µM BSA. The spring constants of the levers were measured using the thermal noise method with NTEGRA Prima scanning probe microscope (NT-MDT, Russia). Results from the experiment series were processed to PDFs in a MatLab™ (MATH WORKS, USA) [109] and [110].

In the experiments, solid-phase antibodies (monoclonal anti-TSH antibody 5409, Medix Biochemica) were covalently bound to mica in a three-step procedure. First, freshly cleaved muscovite mica was aminofunctionalized using 3-aminopropyltriethoxysilane (APTES, Sigma) in the gas phase [111] and [112]. Secondly, a 50 µl droplet of 1 mM ethylene glycol-bis(succinimydylsuccinate) (EGS, Pierce Biotechnology) in 50 mM NaH_2PO_4-buffer at pH 7.0 was added to the aminofunctionalized mica. Thirdly, after 5 minutes incubation 50 µL of 50 mM NaH_2PO_4-buffer at pH 7.4 containing 200 ng of the solid-phase antibody was added and allowed to react for 25 minutes. Finally, 500 µg of BSA in 50 µl buffer A was added to block the rest of the EGS-functionalized mica. The solid-phase surface was washed five times with TSA buffer (100 mM Tris, 150 mM NaCl, and 7.7 mM NaN_3) to inactivate unreacted EGS. [**III**]

4.6. Biolayer interferometry biosensors

Association kinetics in [**III**] was measured with Octet RED384 biolayer interferometry biosensor (FortéBio, Pall Life Sciences, US) using streptavidin probes (FortéBio, Pall Life Sciences). In the Octet biolayer interferometry system, the target antibody was immobilized on the functionalized tip of a fiber optic probe that is dipped into TSH solution and further to nanoparticle suspension to observe association kinetics. First, the SA-sensors were allowed to hydrate and stabilize in Kbuffer ((50 mM Tris–HCl (pH 7.8), 150 mmol/l; NaCl, 7.7 mmol/l; NaN3, 75 µM BSA, Tween 40, small amounts of different nonspecific IgGs and chelates for divalent cations) Kaivogen, Turku Finland), which was used throughout the experiment series

for dilutions and suspensions. The saturating concentration (190 µM) of biotinylated anti-TSH5409 Mab was incubated for 20 min onto the streptavidin probes and washed for 5 min. Then, the analyte TSH was added in the concentration of 500 mIU/l in the case of specific binding and excluded from the nonspecific case. The incubation time for the analyte was 25 min. The sensors were then washed for 5 minutes in Kbuffer. Finally, the association of anti-TSH5404 Mab coated bioconjugate nanoparticles [**II**] was recorded for 4 hours. Bioconjugate nanoparticles were used in suspensions of 3×10^8, 1×10^8, 3×10^7, 1×10^7 and 3×10^6 particles/µl. The experiment was performed at 30°C using the default settings of the instrument and stirring speed of 1000 rpm. The raw interference signal phase shift change was negative upon nanoparticle binding, due to the size of the nanoparticles. The signal was inverted to positive from nanoparticle binding onward to allow fitting according to exponential association function.

The electron micrographs were acquired from biofunctionalized gold sputtered AFM-probes with a surface scanning electron microscope (SEM) ZEISS 1540XB CrossBeam high resolution GEMINI®-system. Force measurements, using AFM tips functionalized with anti-TSH5404-BSA–coated nanoparticles, were performed on solid-phase bound anti-TSH5409 antibodies in the absence and presence of thyroid-stimulating hormone (TSH) (30 mIU/l) on an AFM 5500 (Agilent Technologies, USA) setup. Silicon nitride AFM probes (Si_3N_4, MCLT, Veeco) were functionalized with amine groups [114] and [111]. [**III**]

5. RESULTS AND DISCUSSION

We have studied the assay performance and particularly nonspecific binding properties of nanoparticle labels of different sizes using high affinity monoclonal antibodies and recombinant antibody fragments against clinical analytes TSH and PSA. Typically, the following assay procedure was applied: biotinylated capture antibodies or antibody fragments were attached on streptavidin-coated microtiter wells followed by analyte incubation. Biotinylated detector antibodies or antibody fragments were attached onto streptavidin-coated europium(III) nanoparticles in a microtube. Thereafter the nanoparticles were added to the microtiter wells containing the analyte.

5.1. Nanoparticle size

Colloidal stability of bioconjugate nanoparticles is affected by the antibody coating, nanoparticle size and nanoparticle concentration. We then characterized this effect of particle size to colloidal stability and to both specific and nonspecific binding. Five different europium(III) particle sizes were available from the same manufacturer, 23.5, 34, 46, 53.5 and 101 nm in radius. In our experience, the binding of larger particles is considerably weaker in addition they fall well beyond the definition of nanoparticles and thus they were omitted from the study. It has previously been shown that the number of europium(III) chelates within a particle followed in a linear manner the particle volume (Härmä et al., 2001). Size distribution of the SA-coated nanoparticles was determined using photon correlation spectroscopy. All non-coated nanoparticles were stable colloids in suspensions. For streptavidin-coated 23.5 and 34 nm particles, aggregation was observed. In the 23.5 nm bioconjugate nanoparticles the maximum size of aggregates was larger and very few individual particles were seen. In the 34 nm particles some individual particles were seen and the average aggregate size was smaller. The streptavidin-coated particles of 46, 53.5 and 101 nm in radius were stable colloids (Figure 4). The SA-coating increased the particle hydrodynamic radius of all the particles measured.

In the sandwich immunoassay a combination of Fab fragment of anti-PSA 5A10 as the capture antibody and anti-PSA monoclonal antibody H117 as the detector antibody had the highest S/B-ratio. This combination was utilized when the effects of nanoparticle size to assay performance were assayed. The standard curves for PSA assay were run with all particles keeping the number of particles per reaction constant (**I**, Figure 5). As expected, the largest particles with the most Eu-chelates gave the highest overall signals. From the measured standard curves the lowest limit of detection were calculated for each particle size: 34, 17, 6.8, 23 and 115 pg/ml for nanoparticles of 23.5, 34, 46, 53.5 and 101 nm in radius, respectively. With the largest particle a considerable nonspecific binding was observed. In contrast, the smallest particles gave the smallest nonspecific signal. This was expected as the volume and thus also the amount of Eu-chelates was in the largest particle 80-fold higher than in the smallest. The highest S/B-ratio was achieved with a particle of 46 nm in radius or 92 nm in diameter.

Bearing in mind the relation between particle volume and signal output we divided the nanoparticle-based immunoassay signals with particle volumes. This resulted in the number of bound particles in each assay. In the volume-normalized signal of the zero calibrator sample (i.e. the background signal) yielded a statistically non-significant trend in relation to

the particle size, in both PSA and TSH assays (**I**, Figure 5). These results suggest that nonspecific binding was independent of the particle size. However, the specific signals decreased as the size of the particles increased. Therefore the highest S/B-ratio was measured for smaller particles. Deviating from this trend, the S/B-ratio for the smallest particles was significantly lower. This was due to the colloidal instability of the bioconjugate nanoparticles that increased the average particle size and, thus, decreased the specific signal.

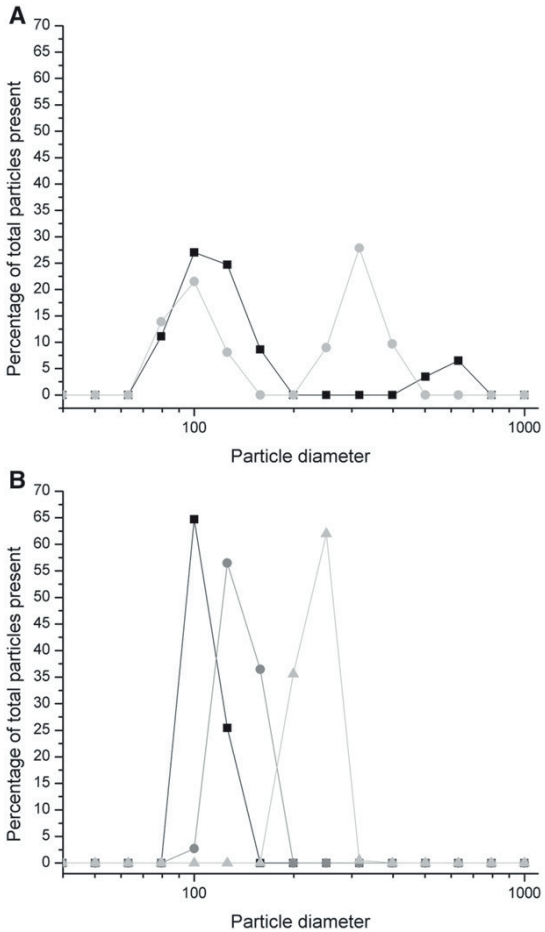

Figure 4. Colloidal stability of the SA-coated nanoparticles. Size distribution curves showed aggregation of the smallest two particles (A) of 23.5 nm (squares) and 34 nm (circles). For the largest three particles (B) of 46 (squares) 53.5 (circles) and 101 nm (triangles) no aggregation was observed.

The difference in the S/B-ratio is carried over to LLD of the assays indicating that the colloidal stability bioconjugate nanoparticles is in direct relation to the LLD of the assay. Here we utilized a relatively high number of nanoparticle labels, 1×10^9 per microtiter wells. This had two direct consequences: the high background signal at a zero analyte concentration and reduced assay sensitivity.

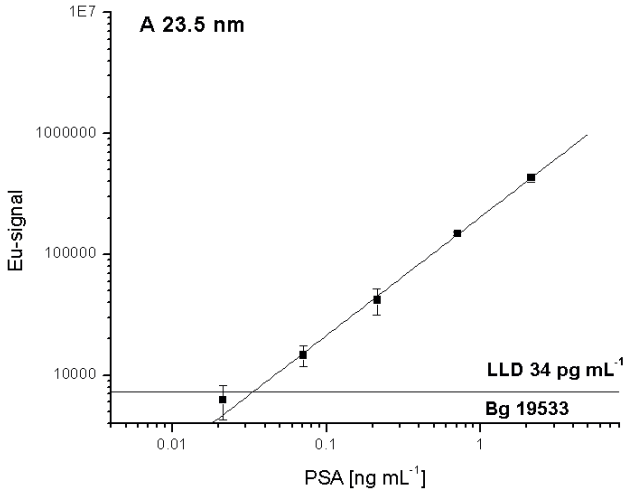
A 23.5 nm
1E7
1000000
100000
10000
Eu-signal
LLD 34 pg mL-1
Bg 19533
0.01
0.1
1
PSA [ng mL-1]

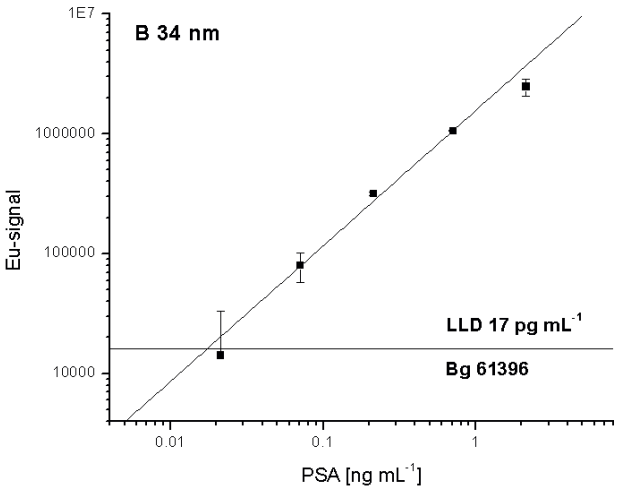
B 34 nm
1E7
1000000
100000
10000
Eu-signal
LLD 17 pg mL-1
Bg 61396
0.01
0.1
1
PSA [ng mL-1]

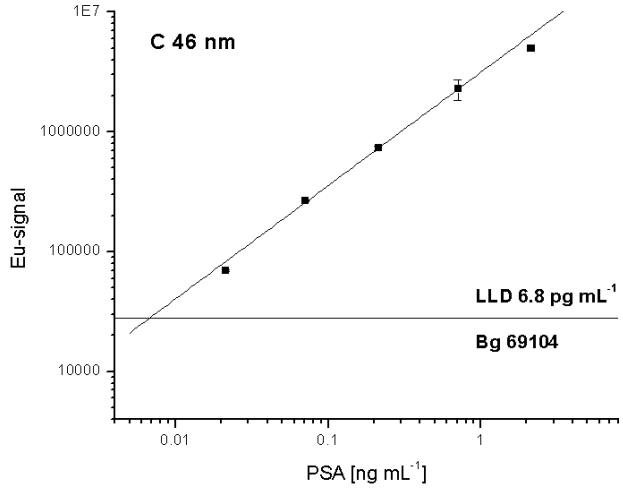
C 46 nm
1E7
1000000
100000
10000
Eu-signal
LLD 6.8 pg mL-1
Bg 69104
0.01
0.1
1
PSA [ng mL-1]

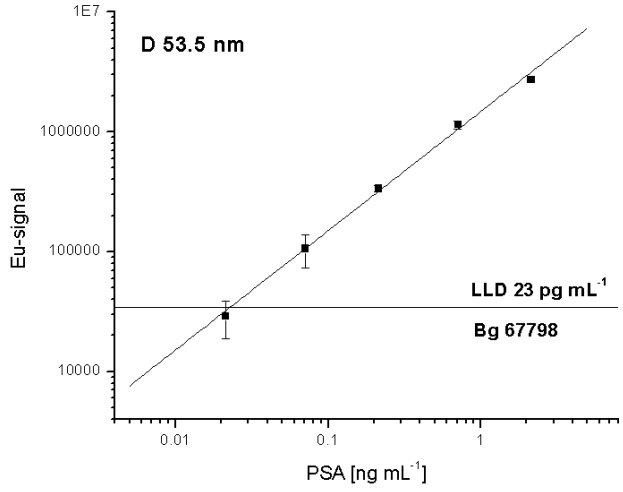
D 53.5 nm
1E7
1000000
100000
10000
Eu-signal
LLD 23 pg mL-1
Bg 67798
0.01
0.1
1
PSA [ng mL-1]

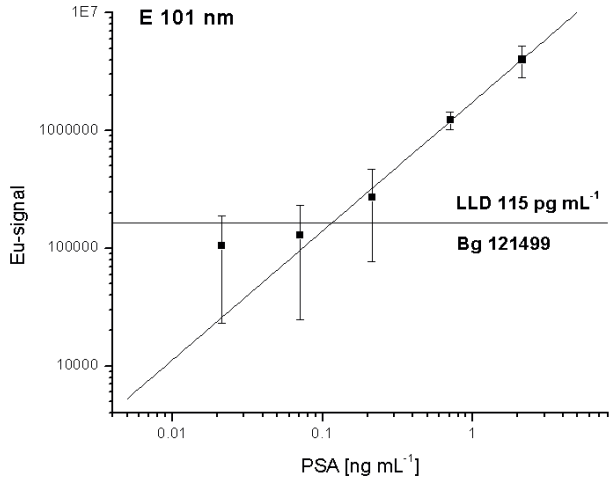

Figure 5. PSA-immunoassay standard curves using nanoparticles labels of 23.5 nm (A), 34 nm (B), 46 nm (C), 53,5 nm (D) and 101 nm (E) in radius. The horizontal lines show the LLD values calculated using 3×SD of the zero calibrator. The Fab-fragment of anti-PSA 5A10 was used as the capture antibody and anti-PSA monoclonal antibody H117 as the detector antibody. The data-points presented are background subtracted and thus the average background signal is set to zero-value and LLD at 3×SD of background. The Bg-value shows the absolute averaged background.

5.2. Antibody type selection in sandwich type assay

Previous studies have shown the importance of the number of binding sites on nanoparticle labels. A high number of binding sites on a nanoparticle increased the probability for analyte binding [23]. Therefore, the number of detector antibody or antibody fragment was optimized to cover densely the nanoparticle surface. The highest S/B-ratio and high signal level in the optimization determined the concentration used in subsequent tests (data not shown). Working at maximum S/B-ratio eliminated possible errors in experimentally defined antibody concentrations and possible differences in activities of different antibody fragments. In the same way, the amount of capture antibodies was optimized onto the microtiter wells coated with streptavidin.

The performance of different antibodies was compared as both capture and detector antibodies. Combinations of Mab and recombinant Fab- and scFv-fragments were tested in TSH immunoassays and Mab and recombinant Fab fragment in PSA-immunoassays. All antibody fragments were site-specifically biotinylated with maleimide PEO_2-biotin 3 nm spacers that gave additional mobility for the biotins. The monoclonal antibodies were randomly biotinylated through lysines and they retained any possible glycosylations. The immunoassays were carried out using 30 and 120 min incubation. As both incubation times gave equal results, the assay with 30 min incubation are presented here.

Typically, the immunoassays utilizing monoclonal antibodies as detector antibodies produced higher specific signals than recombinant antibody fragments in both PSA and TSH assays (Figures 6 and 7). The highest S/B-ratios were achieved with a Fab-fragment as a capture

antibody and a Mab as a detector antibody. The scFv-fragments did not perform well in the sandwich immunoassays. The PSA-immunoassay gave considerably higher S/B-ratios, as the specific signal was higher and the nonspecific signal lower than in the TSH-immunoassay. Typical S/B-ratio in the PSA-immunoassay was 50 while in the TSH immunoassay it was 15 when 1.5×10^{9} analyte molecules (for TSH 66×10^{-12} M or 10 mIU/l and for PSA 75×10^{-12} M) were used. This indicates that the nanoparticle assay performance was largely dependent on the properties of antibodies used. High specific signal level was the predominant factor in determining the S/B-ratio immunoassay. Decrease of nonspecific binding was found not to compensate for simultaneously occurring weaker specific binding.

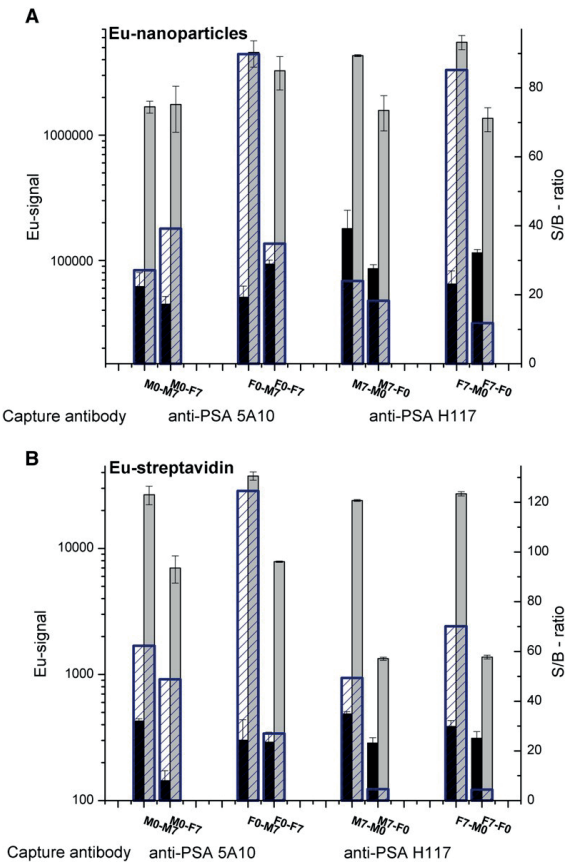

Figure 6. PSA-immunoassays using nanoparticle label (A) and Eu(III) labeled streptavidin (B). Anti-PSA 5A10 (assigned as 0) and H117 (assigned as 7) were used as the capture and the detector antibody, respectively, in the two left set of columns. Anti-PSA H117 and 5A10 were capture and detector antibodies, respectively, in the two sets of columns on the right side. Monoclonal antibodies and Fab fragments are marked as M and F, respectively. Solid bars represent measured europium signals for nonspecific (black) and specific (grey) binding. Transparent bars are S/B-ratios (right y-axis). Error bars are shown in each column. To ensure colloidal stability nanoparticles of 53.5 nm in radius and 1.5×10^{9} PSA molecules (75×10^{-12} M) were used in the assay with a 30-minute incubation time.

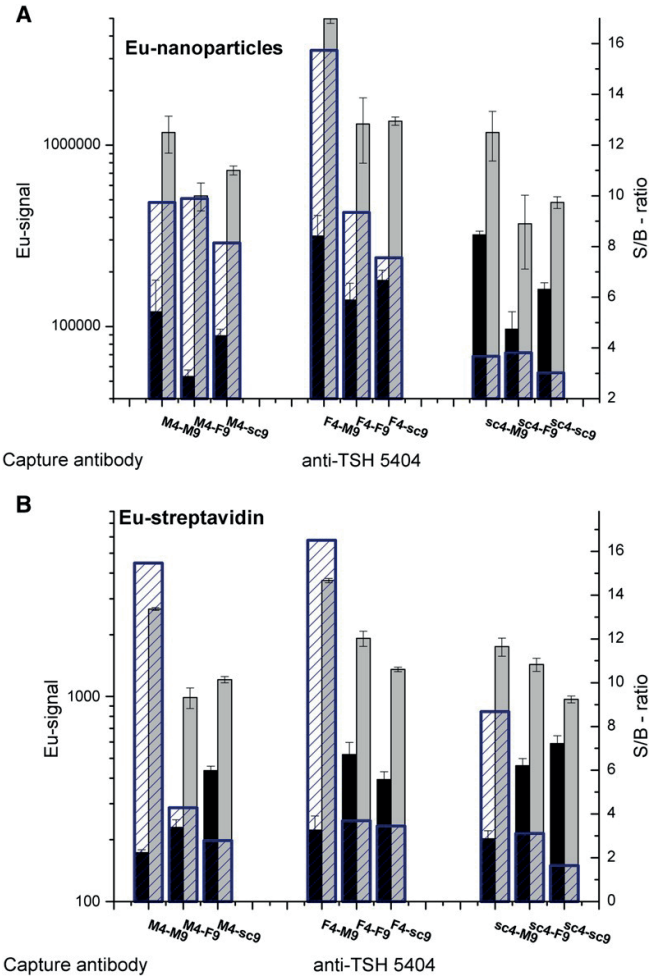

Figure 7. TSH immunoassays using nanoparticle labels (A) and Eu(III) labelled streptavidin (B). Anti-TSH 5404 (assigned as 4) was used as the capture antibody and anti- TSH 5409 (assigned as 9) as the detector antibody. Mab, Fab fragment and scFv are marked as M, F and sc, respectively. Solid bars represent measured europium signals for nonspecific (black) and specific (grey) binding. Transparent bars are S/B-ratios (right y-axis). Error bars are shown in each column. To ensure colloidal stability nanoparticles of 53.5 nm in radius and 1.5×10^9 TSH molecules were used in the assays having an incubation time of 30 min.

Nonspecific binding of Mab was not consistently higher than that for Fab or scFv. These results suggest that removing the Fc-domain does not reduce the nonspecific binding in the buffer-based model immunoassays, neither with molecular labels nor with bioconjugate nanoparticles. This was to be expected as most of the reported Fc-based interferences re present only in clinical samples e.g. the complement [33]. The data suggested that the more favorable orientation of antibody fragments on the capture surface resulted in higher signal and improved S/B-ratio. In addition, the high flexibility of the Mab hinge region, in comparison to antibody fragments, seemed to favor more efficient binding [115], even though the recombinant antibodies possessed a spacer arms to provide them with similar additional mobility. The length of the spacer however, was shorter than the hinge region of a Mab. At the

high particle amount used, no significant difference in nonspecific binding properties of antibody fragments could be concluded from our data. These differences could not be attributed to the number of binding sites as optimized antibody concentrations ruled out large variations in the number of binding sites per nanoparticle label. When only buffer matrix is considered, using Fab-fragments as the capture antibody provided higher S/B-ratios, but in nonspecific binding could not be reduced through antibody fragmentation. Fragmentation may, however, have significant impact in difficult matrices such as blood or serum where autoantibodies or other binding components severely disturb binding events [116].

5.2.1. The effect of the label-type to antibodies

The use of nanoparticle labels was justified by their higher specific activity and higher affinity values in comparison to soluble binders [117]. Therefore, it was interesting to compare soluble europium(III) labeled streptavidin to nanoparticle label using different antibodies and their fragments. As a control the nanoparticle labels were replaced with soluble europium(III)-chelate labeled streptavidin (soluble tracer) (3×10^{11}) in comparative studies. Each labeled streptavidin was measured to comprise 2.4 europium(III) chelates. While the amount of antibodies is roughly equal, the amount of Eu-chelates is hundred-fold less in the control assays using SA–Eu. In our studies, the soluble labels performed nearly identically to nanoparticle labels in all assay setups (Figures 6 and 7). This shows that antibodies used predominately determined the assay performance. This also indicates that the performance of antibodies is independent of the label used for detection. Assays with SA–Eu as a tracer and the nonspecifically biotinylated detector Mabs produced higher signals than those using fragmented antibodies because more than one SA–Eu was bound per antibody.

5.3. Solid-phase stability and coating configuration

Some of the nonspecific binding is speculated to originate from denatured antibodies [76], [30] and [31]. Upon adsorption, antibody's conformational changes can expose amino acids that are attracted to surrounding biomolecules or solid surfaces and thus lead to nonspecific binding. This hypothesis was examined by subjecting the capture antibodies to denaturing conditions using heat, acid and detergents. Experiments were performed on three different capture surfaces: monoclonal antibodies passively adsorbed on microtiter wells and biotinylated Mabs and Fab-fragments attached onto microtiter wells coated with SA. The denaturing steps were applied before the TSH analyte incubation.

First, hydrochloric acid at 0.6 M concentration was incubated on the capture surface and binding activity of the capture surface was observed by determining the specific binding in an immunoassay. While most of the specific signal was lost the nonspecific signal was not affected in comparison to the non-treated surface. The layer of passively adsorbed antibodies was more sensitive to denaturation treatments and all specific binding properties were lost whereas biotinylated antibodies attached to SA retained approximately 15% of binding activity. This was a general trend that was consistently observed throughout this study – antibody coating using a SA layer provided more stability against all denaturation methods used. Similar effects have been reported when capture proteins were immobilized on a preadsorbed layer of SA or anti-mouse IgG [75], [118] and [69].

The SA-bound capture surfaces were treated additionally with different potentially interfering

chemicals in high concentrations. We applied as high as 175 mM SDS, 5 M urea, 5 M NaCl, 20% ethanol and found insignificant deterioration of the binding activity of the capture surface at room temperature. However, with divalent cations (4 M $MgCl_2$) a decrease in specific binding activity was seen. With adsorbed Mab the specific signal dropped to the level of the background signal a 1000-fold decrease. On the contrary, under the same circumstances with a capture antibody (biotinylated Fab-fragment of the same antibody clone) attached to SA only a 5-fold decrease in specific signal was observed. Again, in all experiments the nonspecific binding remained at the level of the control assay. Neither did we observe a trend in either direction in the standard deviation between replicates when interfering chemicals were used.

In the next experiment the effect of heat to binding activity was examined. The heating step was carried out in water for 15 minutes. Temperature up to 70 °C was required to have an impact on binding activity of passively adsorbed surface antibodies whereas antibodies bound to a SA-layer required 80 °C for decreased binding activity (Figure 8 A). To assess the stability of the Fab-fragment we examined the effect of heating to the antibody and the binding of both biotinylated Fab and Mab antibodies in solution. Antibodies were heated up to 90 °C, cooled, diluted into assay concentration, analyte was bound, the complex was immobilized onto SA-surface and the amount of bound TSH was detected with the anti-TSH nanoparticle labels. Both were found to maintain their binding activity after heat treatment in 90 °C water within 20 % deviation from the original activity.

5.3.1. The effect of binder distance from the surface on antibody stability

In denaturing experiments a correlation between stability and distance of the binding domain was observed. The passively adsorbed monoclonal antibody is attached in random orientation and considering its approximate dimensions, length 12 nm, width 15 nm and depth 4 nm [119] and [105] the estimated average distance of the hypervariable region from the surface is around 7 nm. The Fab-fragments were site-specifically biotinylated (with 3 nm spacer) from the end opposite to the hypervariable region and dimension of length 10 nm, width 4 nm and depth 4 nm. The layer of streptavidin had a thickness of around 5 nm [120], but the orientation of the 4 binding sites cannot be controlled. However, we can assume that antibodies attached to it were preferentially directed away from the surface due to site-specific functionalization. In the case of biotinylated Mab, such assumption cannot be made, however, we expect the average distance from the solid-phase to be longer than the Fab-fragment. Thus, the estimated distances of binding sites are 7 nm, 14 nm and 16 nm from the solid-phase for adsorbed Mab, SA-Fab and SA-Mab respectively. In the experiments where heating of capture solid-phases was performed in the presence of 20 mM SDS solution, the denaturation of the capture antibodies on the surfaces was more pronounced and it was observed 20 – 40 °C earlier than with water only (Figure 8B). As the capture surface lost specific binding, also the nonspecific binding decreased, but this was in lesser extent. In all heating experiments the change in nonspecific binding signal was not significant indicating that denaturation of capture antibodies is not a major cause of nonspecific binding in immunoassays. The experiments also show that the antibodies were very stabile even in high temperatures.

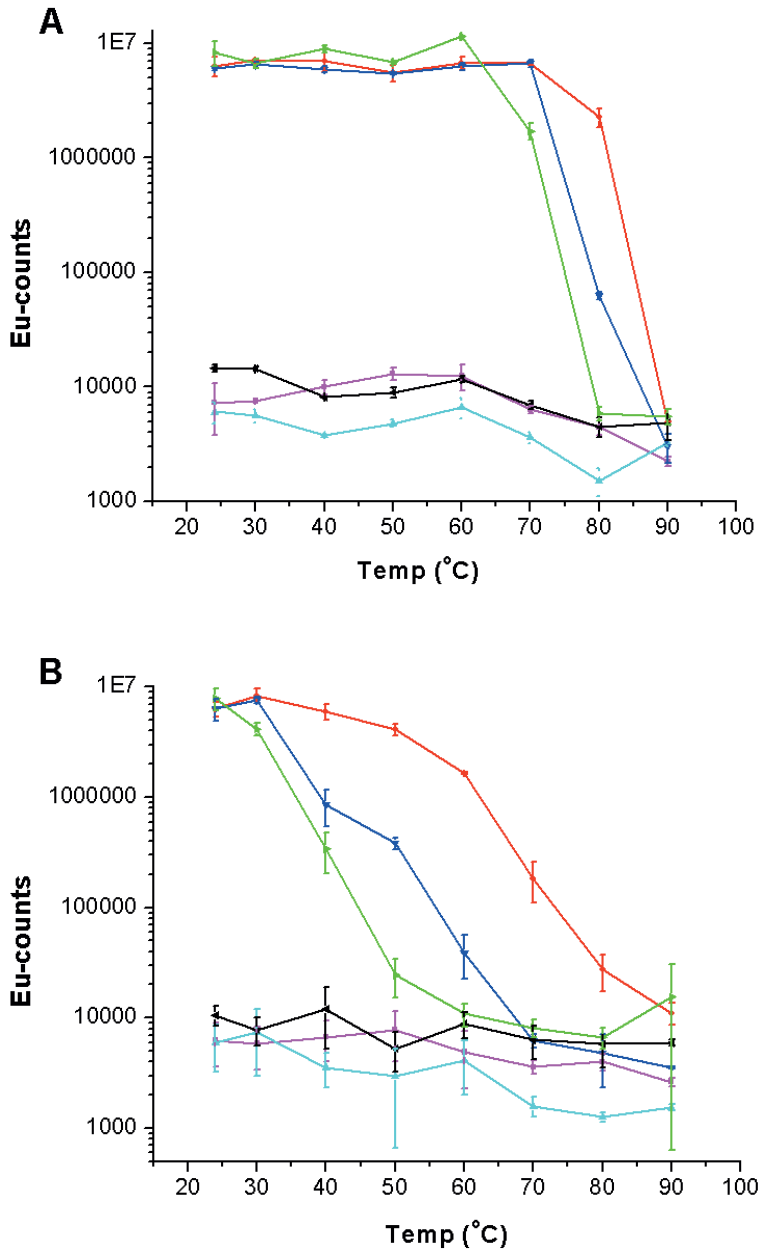

Figure 8. Heat denaturation test of passively adsorbed Mab (signal green; bg. black), and bio-Fab (signal blue; bg. cyan) and bio-Mab (signal red; bg. magenta) captured through SA on the polystyrene surface. The heat treatment denatured passively adsorbed mAb at lower temperature compared to bio-Mab capture on the surface through SA. Heat denaturation was less pronounced in water (A) than with 20 mM SDS (B). The nonspecific binding of nanoparticle labels did not increase when surface-bound Mabs suffered from denaturation.

When protein is adsorbed onto a surface the bonds holding it in place are mostly hydrophobic or hydrophilic in nature. In order to form strong hydrophobic interactions the protein is likely to undergo significant conformational rearrangement, i.e. denature, at least at the contact area. With fairly large proteins e.g. IgG denaturing leads to loss of binding sites on the surface in a considerable fraction of adsorbed protein [69]. The loss of binding activity by denaturation of adsorbed antibodies can be compensated by adding more antibodies to the well. We and others have shown that there is an optimum amount for solid-phase capture antibody [48] and [**I**]. After the optimum has been reached any further addition of the antibody to the well leads to a higher background signal in the immunoassay. To eliminate this source of background coating by passive adsorption should be avoided due to the denaturing effect near the surface. The binders were more resistant to denaturing treatments (stability: ads Mab < SA-Fab < SA-Mab) the further away from the solid-phase surface their binding sites were (7 nm, 14 nm and 16 nm, respectively) (Figure 8B). This suggests that when possible an additional spacer protein or linker should be added when capture surfaces are coated with proteins. Furthermore, in antibody engineering special consideration should be placed also on the stability of the antibody fragments [76]. The loss of binding activity of the Fab-fragment was observed at slightly lower temperatures than the distance from the solid-phase would predict. This could be caused by the less stable structure of the fragmented antibody or the flexible linker that would allow the fragment to bend parallel to the surface. Especially in the case of scFvs the absence of disulfide bonds is likely to cause decreased stability of the fragments. Especially with nanoparticulate labels and solid-phases, use of stabile binders produce higher specific signals outweighing minor improvements in the level of nonspecific background signal.

5.4. Binding kinetics in nanoparticle assay

Kinetic differences between specific and nonspecific binding in the well plate format PSA-immunoassay utilizing nanoparticle labels were tested in relation to particle size. Diffusion speed decreases as particle size increases and so the assay kinetics was assumed to slow down when larger nanoparticle labels were used [65]. This was studied by incubating nanoparticle bioconjugates of different size for 120, 240, 480 and 1140 min. The S/B-ratio was at the maximum at 120 min for all particles. Longer incubation times gave higher signals, both specific and nonspecific. Saturation of the specific signal was observed for 53.5 and 101 nm particles at 480 min, for 46 nm particles at 240 min and for 34 nm particles at 120 min, thus the nanoparticle size had an apparent impact on assay kinetics. The signal for nonspecific binding increased steadily over the whole incubation time up to 1140 min. This increase led to lower S/B-ratio, suggesting as expected that the specific binding is faster than nonspecific.

5.4.1. Kinetics of specific binding

Slower kinetics is mainly due to slower diffusion caused by their larger size as compared to molecular labels [26]. In order to characterize the binding constants in more detail we conducted BLI and FS experiments. The specific binding profile is simple single component adhesion (Figure 9A). The K_d of specific binding of the bioconjugate nanoparticle to the solid-phase captured TSH was measured to be 2.5×10^{-11} M compared to the 1×10^{-10} M given by the provider for single Mab (Table 5). The kinetic constants were calculated by running a global fit of the concentration series [67]. The association rate (constant) k_{on} of specific binding was measured to be 6.45×10^{6} M^{-1} s^{-1} and dissociation rate (constant) k_{off} was determined to be

below 1.6×10^{-4} s^{-1}. However, the k_{off} was so low that the dissociation could be considered too slow to be measured and also the standard error for k_{off} parameter was very high. This was mainly due to instrument drift, probably caused by buffer evaporation and slow sedimentation of the nanoparticles. In binding without TSH being present, the bioconjugate nanoparticles had much slower association rate throughout the measured time range, and the association rate constant could only be determined with the two highest nanoparticle concentrations. The majority of the association was occurring during the first few seconds and the reaction was found saturated by 60 s in all the concentrations used (Figure 9B). In well plate assay the binding without analyte shows two-components; at first fast binding is observed and later gradually increasing component dominates, whose inclination remains constant until the reaction is stopped (**III** Figure S1).

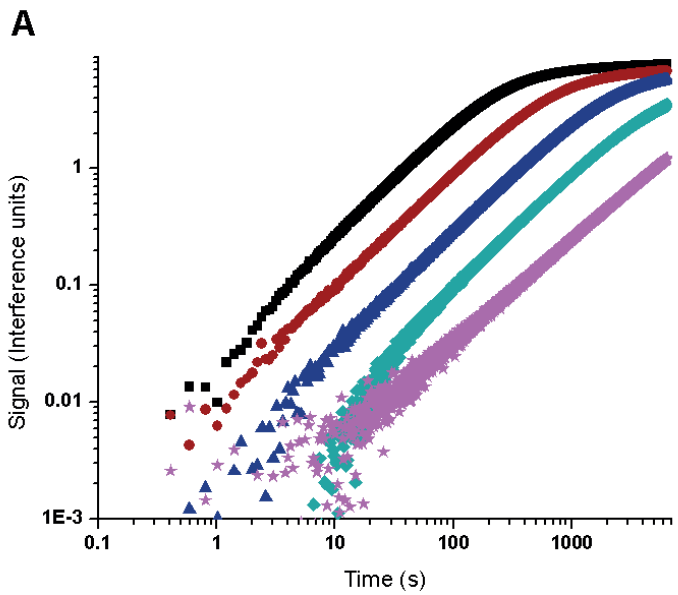

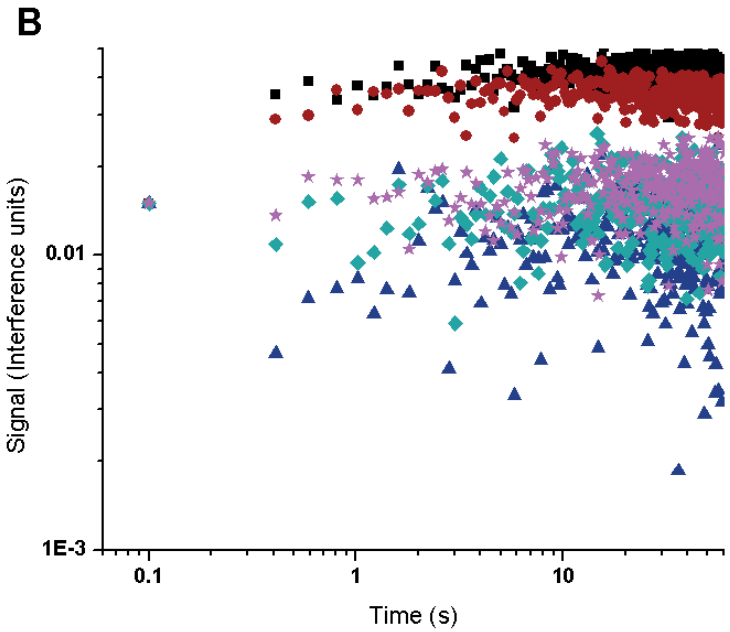

Figure 9. A Log-log plot of binding with 500 mIU L^{-1} TSH (A) and without TSH (B) biosensor binding signals measured with ForteBio Octet RED384. Bioconjugate nanoparticles were used in suspensions of 3×10^8 (■), 1×10^8 (•), 3×10^7 (Δ), 1×10^7 (⬥) and 3×10^6 (*) particles μL^{-1}. Please note the difference in axis scales. The binding with TSH shows strong, fast, single component association. Binding without TSH adhesion shows a very small and fast initial increase with the two highest concentrations and saturation during the first 10 s of the measurement, and then considerably slower signal increase matching background level for the remaining duration of the measurement time (**III**).

To characterize the kinetics on shorter time scales a FS measurement setup was utilized, a sandwich-type immunoassay was performed between a single antibody-functionalized nanoparticle mounted on the outer apex of an AFM tip, TSH and solid-phase antibody bound on a solid mica support (**III,** Figure 2). Similar sandwich-type immunoassay was run on Octet RED384-sensor and standard well plate assay. The combined data from these experiments reveal binding kinetics over a time range from 50 ms to 240 min.

5.4.2. Binding probabilities and bond loading rates

As expected, in the experiments with TSH the binding probability (Figure 10 and **III**, table 1S) and the most probable unbinding force ((MPUF), unbinding force of the highest peak in the PDF) were both higher than in binding without TSH (Figure 10). The MPUF increased 60-80 pN in specific binding (Figure 11) (**III**). The measured anti-THS – TSH unbinding forces were similar to previously described antibody-antigen interactions at the investigated loading rate range [122] and [123]. In FS with bioconjugate nanoparticle probes the specific binding probability was 2-4 times higher [122] and the nonspecific binding probability was 2 times higher [124] or equal [125], when compared to the similar receptor ligand system using conventional single molecule FS. This is due to the relatively large surface area of biologically coated nanoparticles and high density of antibodies. Thus, in nanoparticle FS several bonds may form simultaneously. Moreover, because of the probability of unbinding is roughly equal between the solid-phase antibody – TSH and the tracer antibody – TSH –bonds, some of the

TSH molecules may accumulate on the nanoparticle and further increase the binding probability. Also, the wide probability distribution seen with specific binding (Figure 11A) is likely to be a result of different affinities of the antibodies used. The tracer antibody (clone 5404) had a K_d of 1×10^{-10} M and the solid-phase antibody (clone 5409) had a K_d of 1×10^{-9} M. Although the affinities were different, we were not able to differentiate between unbinding of the two antibody clones in the tracer antibody–TSH–solid-phase antibody – complex.

Bond loading rate

Experiments utilizing nanoparticles were limited to a narrow range of loading rates 5000-30000 pN s^{-1} due to rolling and re-association of the nanoparticle as a consequence of slow probe speed and increased hydrodynamic noise due to high speed of the coated probe (data not shown). At the slower end of the loading rates the specific binding probabilities were close to 100 % and the nonspecific binding probabilities were 40% even at short contact times. In addition, the force distribution at slow loading rates was not shifted to lower forces as is usually observed in conventional FS, but remained between 35-60 pN in both specific and nonspecific binding (Figure 11). In those experiments where the probe contact time with the solid-phase was decreased, an increase of unbinding force was observed. Typically such an increase is seen when probe speed, a variable commonly utilized to increase the loading rate, is increased. We speculate that this is caused by rolling and fast re-association of the bioconjugate nanoparticle.

5.4.3. Association rate

Changing the probe contact time with the solid-phase allows studies on the association of bioconjugate nanoparticle binding to a biofunctionalized solid-phase. The binding probability here describes the number of binding events and hence allows an estimation of the association rate to be made. The binding probability closes to zero as contact time of probe and solid-phase is shorter than the association rate. As expected, we observed an overall decrease of binding probability over the used contact time range investigated. In a two-tailed t-test that allowed unequal variance between samples was found a significant difference in contact times below 100 ms (Figure 10 and **III**, table 1S). We chose to average binding probabilities measured by varying loading rate to exclude the effect of probe velocity. If both, the loading rate and contact time, were kept constant a significant difference (two tailed t-test significance p-value < 0.01) was seen in all contact time ranges.

The difference in binding probability between binding with and without TSH analyte was found to be significant (p-value <0.05) suggesting that contact times in the low millisecond range may prevent bonds responsible for nonspecific binding being formed in the case of bioconjugate nanoparticles. Short contact times will, however, reduce the absolute signal levels in samples with TSH as well. In the contact time range used in this study, there was a linear increase in the log-log plot for both binding types (Figure 10). It was not possible to totally disallow nonspecific binding, but because of the low binding probability and probability decrease towards zero the association can be estimated to require contact time longer than 30 ms i.e. 3×10^{1} s^{-1}. We are forcing a single bioconjugate nanoparticle into contact and do not allow diffusion, thus the relation to molar constants is not trivial to establish, but as the particle is brought to direct contact the local concentration is very high. Similar estimation cannot be extrapolated with reasonable accuracy from the fitting for specific binding, however, the association rate would seem to be orders of magnitude higher and in

agreement with the biosensor data (Figure 10). Also, in the binding measurement performed in the presence of TSH (30 mIU L^{-1}) in the FS setup, the overall binding signal is likely to include a component of nonspecific binding of the nanoparticle in addition to antibody-antigen binding.

Table 5. Summary of determined binding constants. The specific binding kinetic constants were measured with BLI and nonspecific data with FS (Figure 9A and Figure 10).

Specific binding kinetics				
Interferometry	Kon / M^{-1} s^{-1}	Koff / s^{-1}	Bmax	Kd / mol L^{-1}
Average	6.45E+06	1.62E-04	8.88	2.51E-11
Std. error	3.50E+04	3.21E-06	0.062	5.97E-13

Nonspecific binding kinetics	
Force spectroscopy	Association / s^{-1}
Average	33
Std. error	4.3

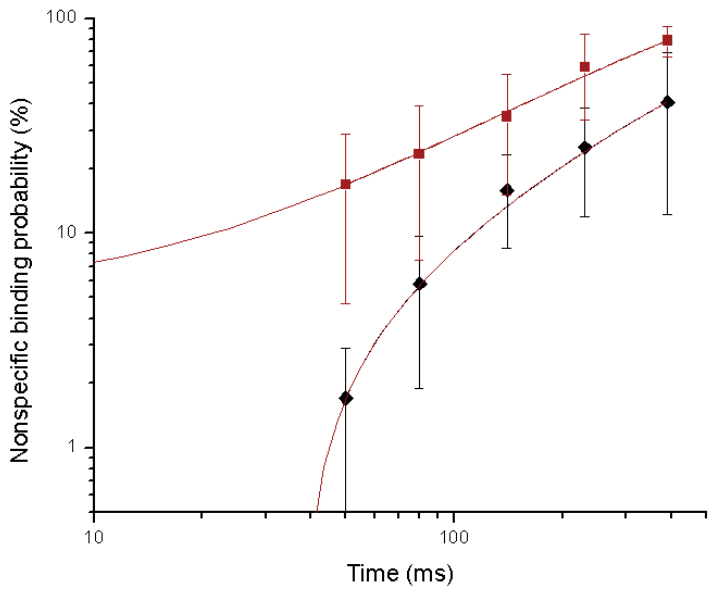

Figure 10. A log-log plot of average binding probabilities for obtained in the presence of TSH (30 mIU L^{-1}) (■) and in the absence of TSH (◆) for bioconjugate nanoparticles versus contact time of the probe and the solid-phase. The binding without TSH appears to be close to zero at contact time 10 - 40 ms, thus binding would happen at rate of 3×10^{1} s^{-1}. The association rate for specific binding cannot be calculated from the data, but would appear to be orders of magnitude higher.

5.4.4. Unbinding forces

No significant difference between the maximum unbinding forces was observed in the experiments performed in the presence or absence of TSH. Therefore, we cannot provide a simple cut-off unbinding force that would separate nonspecific binding from specific. Most probably the measured high binding forces in both experiments (over 300 pN) are caused by nanoparticle adhesion to the substrate via many parallel weaker bonds, thereby creating a strong macro-bond. Such events were rare with probabilities of 0.3% (1-8 out of 1000 force distance curves recorded) or lower. In a previous study similar probabilities for nonspecific binding (0.02-2% of total particles in an assay) were observed in ultrasensitive sandwich-type immunoassay [81].

The changes in the MPUF are an indication of dissociation rate being reached, i.e. applying or loading force on the bond at the same rate as k_{off} (spontaneous water-aided dissociation) would yield no unbinding force at all [126]. However, the MPUF remained between 35-60 pN in both binding with and without TSH, despite the decrease in loading rate. The difference in the MPUF between binding with and without TSH, although clearly distinguishable, was also less than expected. Based on previous affinity constant measurements, this was somewhat surprising, as nonspecific interactions are typically thought to be much weaker than specific binding [127] and [128]. This data indicates similar slow dissociation and overall bond characteristics in both specific and nonspecific binding of bioconjugate nanoparticles. As contact time was decreased, the MPUF was increased. In the binding with TSH the increase was found at contact times shorter than 120 ms and in experiments based on binding without TSH shorter than 95 ms (Figure 11). The increase of the MPUF was from 60 pN to 110 pN with TSH and from 35 pN to 80 pN without TSH (Figure 11). However, the molecular mechanism behind the increase of unbinding force can be similar to the observed unbinding force increase loading rate is increased. The delay, with which the tip-bound nanoparticle follows the movement of the probe, accelerates the speed of the nanoparticle when the direction of the movement is reversed. Nevertheless, the decrease stabilized between 35-60 pN most likely due to avidity of the bioconjugate nanoparticles, continuous dissociation and re-association of bonds maintaining a stable macro-bond.

The majority of unbinding events seemed to resemble a simultaneous unbinding of more than one bond i.e. the binding signal resembled that of a single molecule binding, but the distribution of forces was wider [**III**]. Although in binding with TSH, the analyte concentration allowed a nanoparticle to bind through more than one specific bond, the appearance of only one major peak suggests that the additional binding can also be similar to nonspecific binding. Distributions of binding forces in cases where specific binding is measured were not a simple Gaussian distribution and subsets of binding forces are found. When the contact time was increased more subsets could be fitted into the PDF. In binding without TSH, the unbinding force distribution was more uniform over the contact time range used, but at the shortest contact times distinct subsets emerged. In a previous study such overlapping Gaussian distributions have successfully been resolved [129]. However, nonspecific binding is assumed to comprise several different bond types and thus similar component analysis did not yield a result. Some cases showed the characteristics of zipper-type probe relaxation where the probe was partially relaxed between individual unbinding events. Zipper-type relaxation may be due to nanoparticle rotation upon unbinding. Such a mechanism fits well to the observed tendency of re-association of bonds.

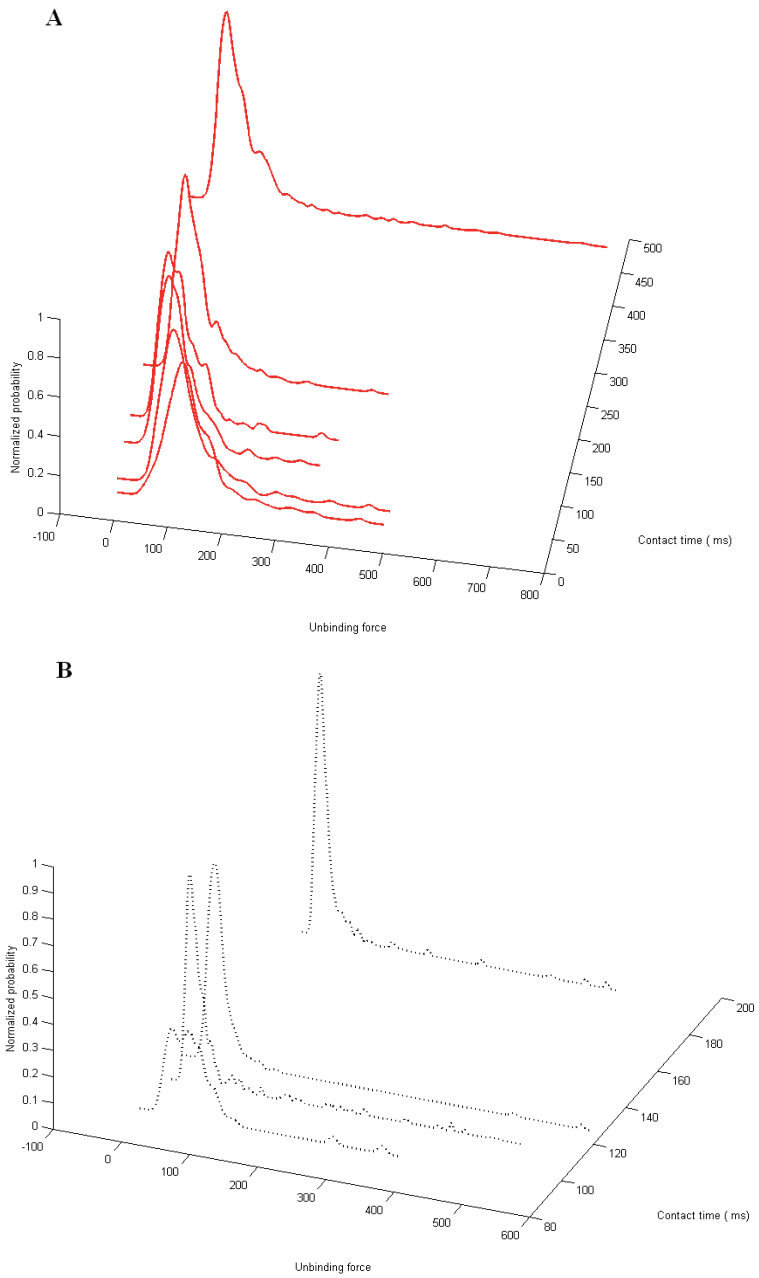

Figure 11. Contact time–dependence of the unbinding forces. Red solid lines (A) show the unbinding force PDFs of binding with TSH (30 mIU/l) and black dotted lines (B) reflect binding without TSH. On the z-axis is the normalized probability, on x-axis the unbinding force [pN], and on the y-axis the probe contact time with the sample in milliseconds. With short contact time in nonspecific case, no unbinding events were detected which was partly due to cantilever vibrations and signal noise caused by the relatively high loading rate.

5.5. Matrix effects

5.5.1. Stabilization of bioconjugate nanoparticle's protein corona

The colloidal stability of bioconjugate nanoparticles is defined by their surface potential, the stability of conjugated antibodies, ionic strength of the assay buffer, detergents in the assay buffer, concentration of bioconjugate nanoparticles in the suspension, presence blocking proteins and the stability of their protein corona. As compared to small molecules, the particles have slower exchange of molecules at their surface. When the bioconjugate nanoparticles are diluted to the assay buffer from a separate storage buffer where they were stored in high concentration the equilibrium of proteins at the surface is perturbed and the system begins to find a new equilibrium. During this process bonds form and break, and this opens a possibility for un-wanted nonspecific interactions. Once the equilibrium of the protein corona is formed such interactions are less likely to form. We discovered that storing bioconjugate nanoparticles in KVG-buffer at concentration no higher than 100-times that of the optimal usage concentration increased the signal-to-noise ratio of the assay nearly 3-fold (Figure 12).

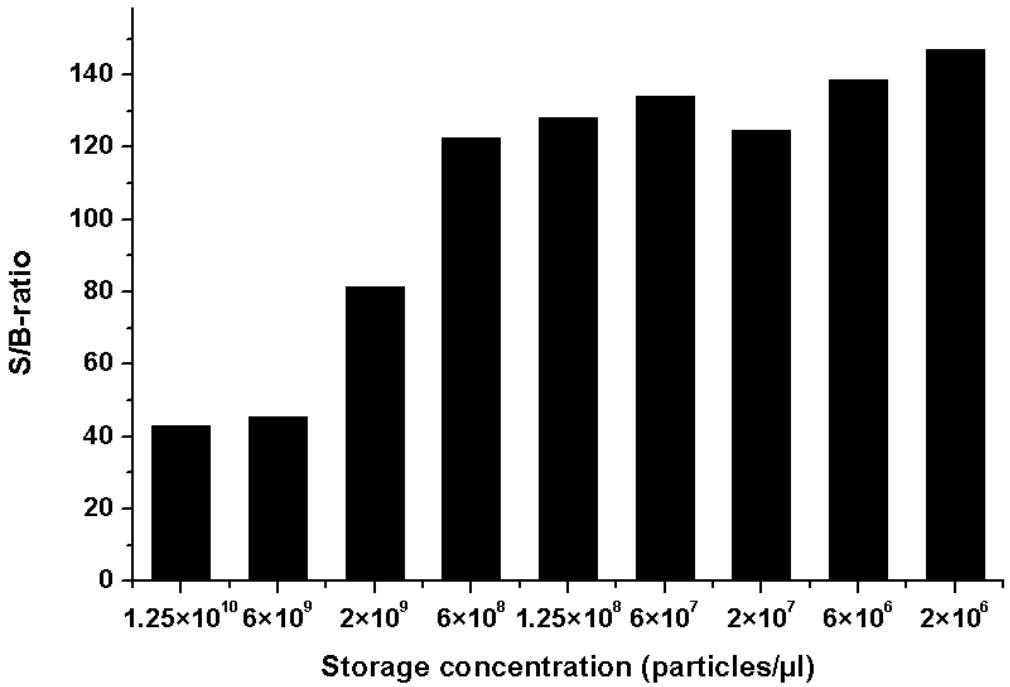

Figure 12. Concentration dependent protein corona stabilization. The bioconjugate nanoparticles were stored in KVG-buffer at various concentrations. The stabilization of the particle suspension was reached at a concentration 100-fold higher than the concentration used in the assay.

To investigate the stabilization in more detail we tested the components of the KVG-buffer to establish, which of the components were required to deliver the effect. We also wanted to test whether the effect was only due to better dispersibility of the more dilute solution or were specific buffer components required for the effect. A component-by-component test of the buffer ingredients was conducted at a concentration of 1.25×10^{8} particles/µl (Figure 13). As expected, the blocking protein BSA was the main component in the buffer during stabilization and that blocking detergent Tween 40 was of secondary importance the main components in the storage buffer. The importance of the detergent subsided slightly when buffer pH was adjusted to the optimal according to the antibody. Nearly a three fold improvement in the S/B-ratio, and the full potential of the stabilization, was reached by using the optimum pH, physiological ionic strength, blocking protein and detergent. However, when these components were added to the storage buffer at particle concentration 1.25×10^{10} particles/µl no benefit was observed.

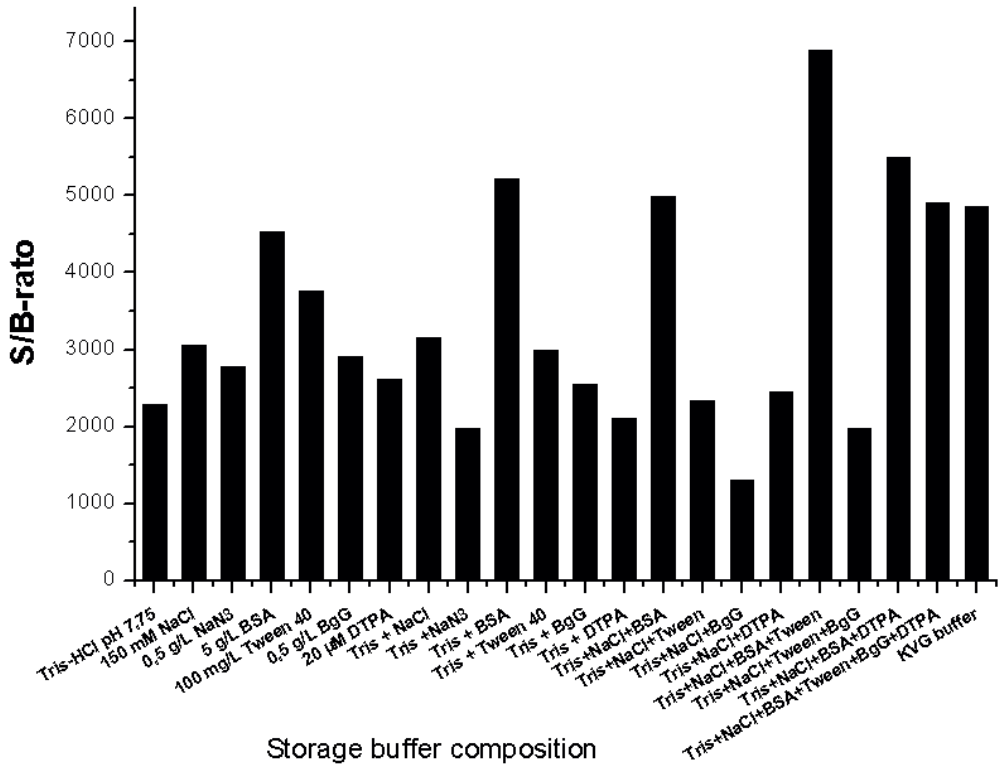

Figure 13. Component-by-component breakdown of the storage buffer composition in concentration of 1.25×10^{8} particles/µl.

5.5.2. Sample pre-processing by affinity purification

The TSH serum samples were prepared by affinity purifying pooled serum samples and later spiking a desired amount of recombinant TSH into the sample. Analyzing these samples we

observed a reduced level of nonspecific background signal from a zero calibrator sample (Figure 14). This would imply that the affinity purification of TSH removed also cross-reactive or interfering compounds from the sample. Removal of such compounds from a clinical sample would naturally make detection of even smaller concentrations of the analyte possible. This could be achieved by a preprocessing step where the sample would be affinity filtered with antibodies (e.g. with antibody coated microbeads) bearing close resemblance to capture and/or detector antibodies, but would not recognize the antigen. In order to quantify the observation we utilized similarly produced anti-PSA 5A10 Fab-fragment – coated wells [**I**] to affinity purify pooled serum samples with low-normal range TSH (approximately 1 mIU/L). We mock affinity purified the female serum with 5A10 Fab-fragments and measured the increase of signal-to-noise ratios with a different amount of diluted serum where 100 µIU/L of recombinant TSH was spiked (**IV** Figure 4). In this experiment, the amount of TSH was fixed in respect to the total volume of buffer and serum, i.e. the serum TSH concentration in 5% sample would be ten times as much as in the 50% sample. We observed that at concentrations over 10% (v/v) the signal-to-noise ratios increased in response to affinity purification. The effect was mainly due to increased recovery of the spiked TSH. The higher the amount of serum in the sample was the stronger effect the affinity purification delivered.

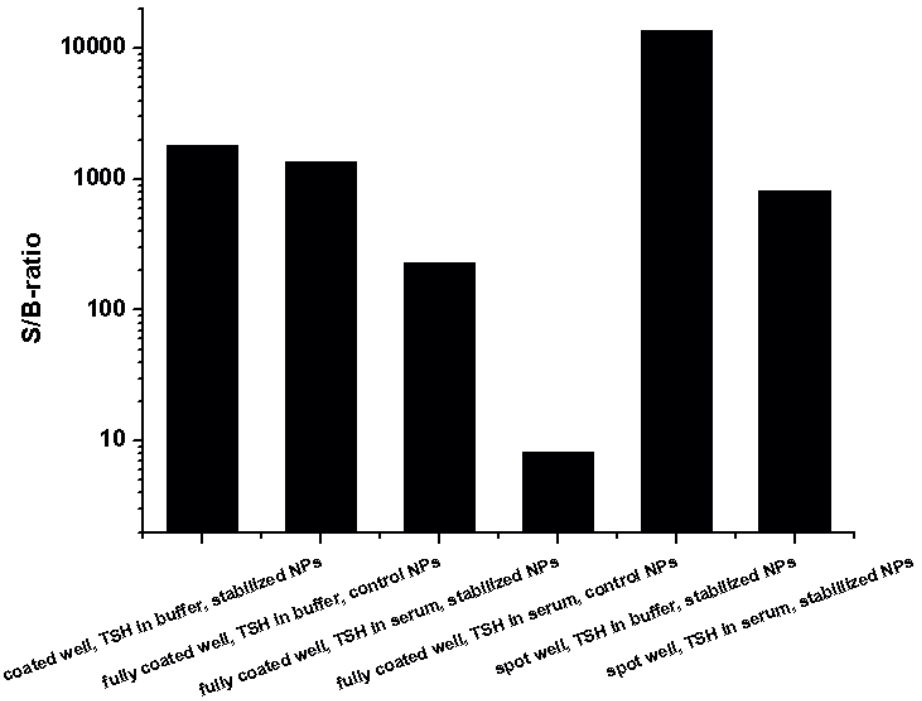

Figure 14. Comparison of TSH-assay S/B-ratios in KVG-buffer and in 50% affinity purified serum. The assay utilized normal and protein corona stabilized bioconjugate nanoparticles and fully coated and spot-coated microtitre wells. The optimized configuration gave 10-fold higher S/B-ratio in KVG-buffer and a 100-fold higher ratio in 50% affinity purified serum.

5.6. Super-sensitive TSH assay utilizing bioconjugate nanoparticles

5.6.1. Control of association time by solid-phase organization

We have shown that the association rate of specific binding of bioconjugate nanoparticles, the k_{on}, is 200000-fold higher than for nonspecific binding. Therefore, in order to disallow sedimentation and nonspecific binding in immunoassays utilizing biocojugate nanoparticle labels, we decided to control the association time with fast liquid flow induced by mixing and a small area for specific binding [130] and [131]. The coating of only the small area of the active solid phase, was produced by adding the capture-antibody in a 1 µl drop halfway between the edge and center of a streptavidin functionalized 96-well plate well. The capture-antibody occupied only a fraction of the available solid-phase and affinity of the bioconjugate nanoparticle towards the solid-phase without antibodies was significantly lower. When compared against a fully coated well the spot-coated wells provided a S/B-ratio increase of 3-10 –fold. Such solid-phase configuration is likely to reduce rolling of nanoparticles that would potentially increase nonspecific binding by allowing more time for the bioconjugate nanoparticles to adhere. Another mechanism, through which an increase could be mediated, is through signal amplification on the measured area and the decrease in the optimal amount of bioconjugate nanoparticles needed for the assay (**IV,** Figure S1). Decrease of the optimal amount was possible because the signal obtained from the nanoparticles was condensed under the excitation beam of the Victor^2-multilabel counter.

5.6.2. Optimized sandwich-type immunoassay

Taking the previously described findings into account we performed a heterogenic sandwich-type TSH-immunoassay utilizing bioconjugate nanoparticle labels in affinity purified pooled human serum. A typical standard curve measured by using three replicates of each calibrator is presented in Figure 15. The LLD 60 nIU/L or 450 aM or 10000 molecules in sample volume of 20 µl was defined as the signal that 3SD of zero calibrator over the signal obtained from zero calibrator. The assay is a one-step configuration where the un-diluted sample is first added and the tracer nanoparticles are added to the same well without a separation step in between. A washing step is required only before the time-resolved fluorescence signal is recorded. The immunoassay requires a total of 40-minute incubation time, a low amount of reagents and is relatively easy to perform.

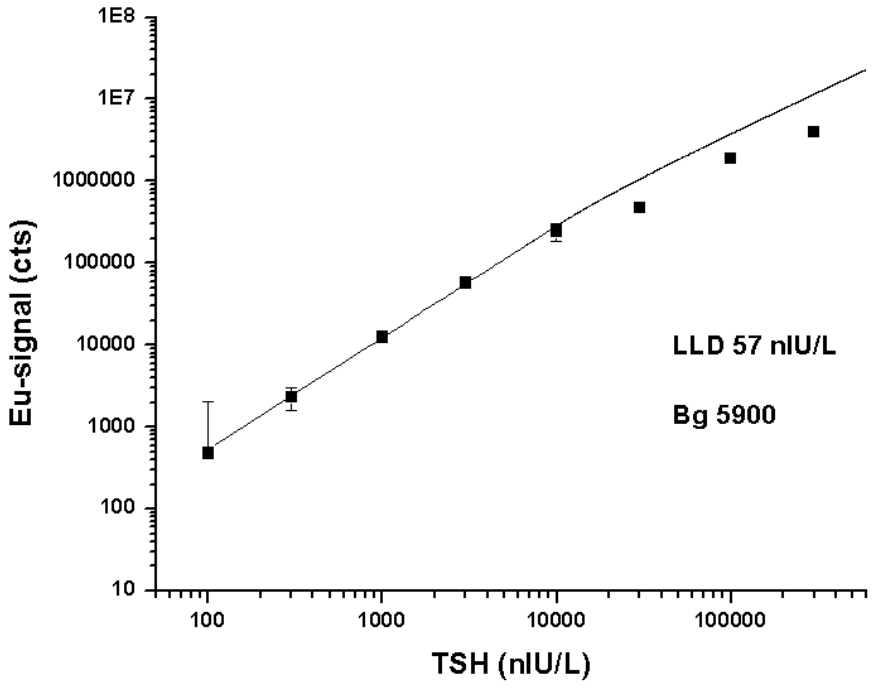

Figure 15. A typical standard curve measured in an affinity purified serum sample by using three replicates of each calibrator. The LLD of the assay was 60 nIU/L or 450 aM or 10000 molecules in sample volume of 20 µl. The data-points presented are background subtracted and thus the average background signal is set to zero-value and LLD at 3×SD of background. The Bg-value shows the absolute averaged background.

6. SUMMARY AND CONCLUSIONS

Nonspecific binding of a detector antibody is often addressed to the Fc-domain of Mab. Fragmentation of detector antibodies did not yield improved performance in buffer-based samples, either when it was used in conjunction with nanoparticulate or soluble labels. A Mab, as both capture and detector antibody, was not found to be the optimal assay configuration. Constantly Fab fragment as a capture and Mab as a detector antibody gave the highest S/B-ratio. The nanoparticle assay performance was largely dependent on the stability and affinity constant of antibodies used. The size of the antibody-conjugated nanoparticles had an insignificant impact on nonspecific binding. While the absolute signal intensity was higher with larger particles, assays utilizing the bioconjugate nanoparticles with a diameter between 65-95 nm gave higher S/B-ratio and lower LLD-value [**I**]. However, bioconjugate nanoparticles smaller than that had a thermodynamic tendency to aggregate, a feature that depends in large extent on the antibody used in the coating. In light of our findings, it appears that in buffer-samples the nonspecific binding in a nanoparticle immunoassay is affected by antibody constant domain, glycosylation or size of the nanoparticle label, only to a very small extent [**I**].

Our data suggests that relatively harsh denaturing conditions are required in order to deteriorate the capture antibody surface. A striking difference in the stability of the capture antibody layer passively adsorbed on polystyrene solid-phase or attached to a streptavidin coated solid-phase via chemically coupled biotin was observed [**II**]. Antibodies attached through SA layer were significantly more resistant to denaturing treatments than those passively adsorbed to the surface. This suggests that the solid surface may act as a "catalyst" and make the antibodies more susceptible to denaturation [**II**] and [69]. Apparently antibody on a capture surface was relatively stable at ambient assay conditions and, therefore, did not create sites on the surface that would promote nonspecific binding of the nanoparticle bioconjugate. In fact, our data shows that nonspecific binding seems not to originate from denatured capture antibodies on surfaces because intentional denaturation of the capture surface did not increase nonspecific binding of the nanoparticle labels. The structural characteristics on the capture surface or denaturation of capture antibody did not promote nonspecific binding. This led us to believe that the addition of sufficient blocking proteins to the capture solid-phase and in assay buffer is sufficient to reduce surface sites susceptible to nonspecific binding [**II**].

In this study the kinetics of specific and nonspecific binding of anti-TSH antibody bioconjugated nanoparticles in a sandwich-type immunoassay were examined with two new methods, biolayer interferometry biosensor and FS. Two novel methods allowed characterizing binding kinetics in time range spanning from 50 ms to 4 h [**III**]. Both methods showed good S/B-ratios compared to single antibodies, due to the avidity and increased K_d of bioconjugate nanoparticles. The k_{off} was shown to be similar for specific and nonspecific binding of bioconjugate nanoparticles, but the k_{on} was 200000-fold higher for specific binding [**III**]. However, we also observed a fast initial nonspecific association of bioconjugate nanoparticles and subsequent saturation and signal decrease in an inverted biosensor method as well as a steady slow increase of signal in well-plate assay that are likely caused by nanoparticle sedimentation. This was despite polystyrene particles having a density equal to water and the nanoparticle suspension being turbidimetrically stable for weeks. We also demonstrated that the maximum unbinding forces in specific and nonspecific binding were nearly equal and even the MPUFs showed only a two-fold difference. This was despite the

orders of magnitude lower affinity constants shown in thermodynamic affinity tests for single antibodies [127] and [128]. Taken together this suggests that controlling the association time with liquid flow (induced with mixing or otherwise) to disallow nonspecific binding and solid-phase orientation to disallow sedimentation could be the optimal strategy to reduce the undesired nonspecific background signal in immunoassays utilizing biocojugate nanoparticle labels [**III**].

A super-sensitive time-resolved FIA for TSH utilizing europium(III) nanoparticle labels with reduced nonspecific binding was developed [**IV**]. The key step obtaining the sensitivity increase was an optimized, spot like, configuration of the active solid-phase that reduced the time a bioconjugate nanoparticle is allowed to roll and associate to an antibody-coated solid-phase [**IV**]. Further, performance enhancement was achieved by stabilization of the protein corona of the bioconjugate nanoparticle label. This was by allowing the protein exchange reactions to reach equilibrium when the particles were diluted or transferred to assay matrix [**IV**]. We also observed that an affinity purification step with an antibody bearing close resemblance to the detector and capture antibody removed interfering compounds from the sample matrix [**IV**]. This is noteworthy as TSH and thyroid hormone assays are especially prone to interferences due to human autoantibodies (HAB) as both Graves' and Hashimoto's diseases are autoimmune disorders [132]. Combined these properties, with previously found general parameters [**I**], [**II**] and [**III**], facilitated the development of a sandwich immunoassay that had a 100 fold lower LLD and increased sensitivity [**IV**].

The developed immunoassay could enable more precise diagnosis and therapy evaluation of metabolic syndrome and pregnancy related thyroid dysfunctions. Graves' (hyperthyroidism) and Hashimoto's (hypothyroidism) diseases are caused by autoimmune disorders [132] and [134]. These conditions are dangerous and may cause congestive heart failure for the mother, miscarriage and impaired cognitive development to the fetus, especially during the first trimester [134]. Thyroid hormones modulate many metabolic pathways relevant to the resting energy expenditure and hypothyroidism is associated with modest weight gain [135]. Positive correlation between TSH and body mass index (BMI) has been documented in number of instances [136]. However, causality of this correlation has not been established TSH synthesis appears to be affected by adipose tissue and caloric intake, highlighted by a study where 98 obese women who over a 6 month period lost more than 10% of body weight, there was a significant decrease in TSH [137]. Conversely, active TSH receptors have been found on adipose tissue [138] and animal tests have identified TSH being involved in lipogenesis [139].

7. ACKNOWLEDGEMENTS

The thesis work was carried out mainly in the Laboratory of Biophysics in the Department of Cell Biology and Anatomy of the Medical Faculty of University of Turku. Smaller portions of it were carried out in the Department of Physical Chemistry in Åbo Akademi and Biophysics Institute of Johannes Kepler University of Linz. I want to express my gratitude for the research infrastructure that has made this thesis possible. I gratefully acknowledge Finnish academy, Tekes and University of Turku (Rectors foundation) for funding the research leading to this thesis.

I want to thank my supervisors Professor Pekka Hänninen and Docent Harri Härmä for your advice and placing your trust and patience on me. With you I have learned many practical skills and valuable lessons about science, teaching, life in the academia, and now I feel that your advice has made me able to stand on my own and further develop my career.

I wish to express my gratitude to the reviewers of this thesis, Professor Niko Hildebrandt and Docent Kristiina Takkinen. You did an awesome effort with very limited time and your scientific insight made the thesis much better. I want to thank Outi, Riitta, Petra, Iris, Christina and Elina from the faculty and department for all the administrative help with the technical issues.

I gratefully wish to acknowledge the co-authors of publications in the thesis Urpo, Markus, Anni, Jouko, Barbara, Vesa, Andreas, Hermann, Ferry and Peter. All of you are phenomenal on your fields of expertise and I have learned a lot from you all. You have made all the publications much stronger and you are among the reasons this thesis ever got printed. I want to thank the group in Linz; especially Andreas and Hermann for all the advice and Constanze, Markus, Miha, Michael L., Martina, Christian, Gerald, Linda, Rong, Josef, Johannes and Isabel for all the fun we had. I, also, thank the biophysics group in Tampere, Vesa and Barbara, the experiments we did with you finally made sense of it all.

I wish to thank co-authors from other publications and collaborators as well, your scientific input has thought me many things, made my research much more versatile and carried me over the moments when this thesis project did not seem to go anywhere. Jessica, Neeraj, Jixi, Didem, Diti, Eva, Tatiana, Sina, Diana, Igor, Veronika and Cecilia, you have broadened my understanding of nanoparticles from *in vitro* –diagnostics to *in vivo* systems, bioimaging, detection and delivery. Petri, Himadri, Anni, Tapani, Marjo, Ronald, Björn, Jawad and Jouko, you have shown how to combine advantages of nano-, microparticles and paper. Riikka, Sami N., Leena, Sami K., Jessica, Tero and Michael S., it has been exiting to measure events inside cells with nanoparticles, and I hope we keep in touch and make our tiny probes even better. Elina, Laura, Mervi, Liisa, Juha, Veli-Matti and Sirkku, for showing us that the work done in the laboratory will make a difference for the benefit of real patients. Oleg, Åsa, Takahiro, Kai-Lan and Kathryn, for the very interesting time spent on trying to figure out how synapses work, we did not find conclusive answers yet so we will certainly keep in touch. Maria, Juha, Miso, Takahiro (again), Elnaz, Jussi, Petri, Gabriela, Madis, Kari V., and Katja, for help in the exciting and surprising field of bone biology, when we tried to understand how the cunning little osteoclasts work. Matthias, Malin, Pirkko, Roope, Juhani, Ilari, Mervi and Jessica, for developing the interesting new prospects in personalized healthcare; we are all individuals, just like everybody else. Also, I thank all the others whom I worked with in countless smaller projects.

I feel much gratitude for the colleagues, past and present, in the Laboratory of Biophysics for the all the fun and the struggles we had in figuring out how things work. Takahiro and Neeraj, I really enjoyed working with you, I feel sad to leave you, but I'm certain that the lab and the projects are left safe, hard-working and skillful hands. Sami K., Kai-Lan, Elnaz, Eija, Mirva, Sari, Kari K., Ezgi, Janne, Alexander and others, keep up the good work. Thank you all! For all help with the glassware and broken things in Medicity thank you Pirjo and Ioan.

I wish to thank the crew in Turku Bioimaging and CIC; Jhon, Diana, Annika, Pasi, Jouko S., Markku, Joanna, Petra M., Eeva, Maritta and all the students, it has been a thrill to see the infrastructure develop, the M.Sc. programme take off and to experience the new talents take off on their wings. My gratitude goes also to the best graduate school in Finland the ISB, Fredrik, Mark and others, through you I have got to know many excellent researches some whom instrumental in completion of this thesis, all whom great fun to be with.

A special thanks to my friends that have taken my mind off science, into football played and watched, trips to Savonlinna to play elephant soccer, to pints we shared and all the laughs. Cheers!

To my parents, Päivi and Seppo, thank you for the love and support, stressing the importance of education, believing in me, and all the advice that have gotten me this far. I thank my mother for insisting integrity and showing the many beautiful tings in the nature. I thank my father for encouraging my interest in mathematics and natural sciences, but first and foremost for pointing out that one must speak one's mine when the opportunity presents itself, to show one's emotions and to make me realize that family matters, and family needs to be cherished. I want to thank my siblings as well, Teemu, Tiina and Anna you are all dear to me. My grandfather Kalevi, thank you for all the times spent in Karuna, fishing trips and mushroom picking, I hope I can share the skills learned from you with my son.

The most sincere gratitude and love I have for my family, my wife Katja and children, Joonatan and Kiia. Katja, it is you that matter the most to all of us, you are the heart of the family, and none of this would ever have been possible without you. I could not have wished for a better companion for my life, you keep making me happy. My son Joonatan, it is amazing to watch you live and learn. Your unconditional love, your inquisitiveness and your bravery all make you one of the most interesting persons I have ever met. Kiia, I have not known you long, but we all waited anxiously to meet you. I love you all.

Tuomas Haarala

27th of June 2014

8. REFERENCES

1. Yalow RS, Berson SA (1959) Assay of plasma insulin in human subjects by immunological methods. Nature 184 (Suppl 21):1648–1649.

2. Ekins RP (1960) The estimation of thyroxine in human plasma by an electrophoretic technique. Clin Chim Acta 5:453–459.

3. Wide L, Bennich H, Johansson SG (1967) Diagnosis of allergy by an in-vitro test for allergen antibodies. Lancet 2:1105–1107.

4. Miles LE, Hales CN (1968) Labelled antibodies and immunological assay systems. Nature 219:186–189.

5. Kricka LJ (1994) Selected strategies for improving sensitivity and reliability of immunoassays. Clinical Chemistry 40:347–357.

6. Ekins RP, Chu F (1994) Developing multianalyte assays. Trends Biotechnol 12:89–94. doi: 10.1016/0167-7799(94)90111-2

7. Wild D (2005) The Immunoassay Handbook. Gulf Professional Publishing

8. Dandliker WB, Schapiro HC, Meduski JW, et al. (1964) Application of fluorescence polarization to the antigen-antibody reaction. Theory and experimental method. Immunochemistry 1:165–191.

9. Dandliker WB, Alonso R, Meyers CY (1967) The synthesis of fluorescent penicilloyl haptens and their use in investigating “penicillin” antibodies by fluorescence polarization. Immunochemistry 4:295–302.

10. Engvall E, Perlmann P (1971) Enzyme-linked immunosorbent assay (ELISA) quantitative assay of immunoglobulin G. Immunochemistry 8:871–874. doi: 10.1016/0019-2791(71)90454-X

11. Van Weemen BK, Schuurs AHWM (1971) Immunoassay using antigen-enzyme conjugates. FEBS Lett 15:232–236.

12. Leif RC, Thomas RA, Yopp TA, et al. (1977) Development of instrumentation and fluorochromes for automated multiparameter analysis of cells. Clin Chem 23:1492–1498.

13. Coons AH, Creech, Jones (1941) Immunological properties of an antibody containing a fluorescent group. Proc Soc Exp Biol Med 47:200–202.

14. Coons AH, Creech HJ, Jones, Berliner (1942) The demonstration of pneumococcal antigen in tissues by the use of fluorescent antibody. J Immunol 45:159–170.

15. Ekins RP (1989) Multi-analyte immunoassay. J Pharm Biomed Anal 7:155–168.

16. Tozzoli R, Bagnasco M, Giavarina D, Bizzaro N (2012) TSH receptor autoantibody immunoassay in patients with Graves’ disease: improvement of diagnostic accuracy

over different generations of methods. Systematic review and meta-analysis. Autoimmun Rev 12:107–113. doi: 10.1016/j.autrev.2012.07.003

17. Hall M, Kazakova I, Yao YM (1999) High sensitivity immunoassays using particulate fluorescent labels. Anal Biochem 272:165–170. doi: 10.1006/abio.1999.4155

18. Härmä H, Soukka T, Lönnberg S, et al. (2000) Zeptomole detection sensitivity of prostate-specific antigen in a rapid microtitre plate assay using time-resolved fluorescence. Luminescence 15:351–355. doi: 10.1002/1522-7243(200011/12)15:6<351::AID-BIO624>3.0.CO;2-3

19. Schultz S, Smith DR, Mock JJ, Schultz DA (2000) Single-target molecule detection with nonbleaching multicolor optical immunolabels. Proc Natl Acad Sci USA 97:996–1001.

20. Zijlmans HJMAA, Bonnet J, Burton J, et al. (1999) Detection of Cell and Tissue Surface Antigens Using Up-Converting Phosphors: A New Reporter Technology. Analytical Biochemistry 267:30–36. doi: 10.1006/abio.1998.2965

21. Frank DS, Sundberg MW (1981) Fluorescent Rare Earth Chelate in Polymeric Latex Particles.

22. Pei X, Zhang B, Tang J, et al. (2013) Sandwich-type immunosensors and immunoassays exploiting nanostructure labels: A review. Analytica Chimica Acta 758:1–18. doi: 10.1016/j.aca.2012.10.060

23. Soukka T, Härmä H, Paukkunen J, Lövgren T (2001) Utilization of kinetically enhanced monovalent binding affinity by immunoassays based on multivalent nanoparticle-antibody bioconjugates. Anal Chem 73:2254–2260.

24. Hou J-Y, Liu T-C, Lin G-F, et al. (2012) Development of an immunomagnetic bead-based time-resolved fluorescence immunoassay for rapid determination of levels of carcinoembryonic antigen in human serum. Analytica Chimica Acta 734:93–98. doi: 10.1016/j.aca.2012.04.044

25. Hucknall A, Kim D-H, Rangarajan S, et al. (2009) Simple Fabrication of Antibody Microarrays on Nonfouling Polymer Brushes with Femtomolar Sensitivity for Protein Analytes in Serum and Blood. Adv Mater 21:1968–1971. doi: 10.1002/adma.200803125

26. Kankare J, Vinokurov IA (1999) Kinetics of Langmuirian Adsorption onto Planar, Spherical, and Cylindrical Surfaces. Langmuir 15:5591–5599. doi: 10.1021/la981642r

27. Davies J, Roberts CJ, Dawkes AC, et al. (1994) Use of Scanning Probe Microscopy and Surface Plasmon Resonance as Analytical Tools in the Study of Antibody-Coated Microtiter Wells. Langmuir 10:2654–2661. doi: 10.1021/la00020a026

28. Allen S, Connell SDA, Chen X, et al. (2001) Mapping the Surface Characteristics of Polystyrene Microtiter Wells by a Multimode Scanning Force Microscopy Approach. Journal of Colloid and Interface Science 242:470–476. doi: 10.1006/jcis.2001.7800

29. Ylikotila J, Hellström JL, Eriksson S, et al. (2006) Utilization of recombinant Fab fragments

in a cTnI immunoassay conducted in spot wells. Clinical Biochemistry 39:843–850. doi: 10.1016/j.clinbiochem.2006.04.023

30. Wörn A, Plückthun A (2001) Stability engineering of antibody single-chain Fv fragments. Journal of Molecular Biology 305:989–1010. doi: 10.1006/jmbi.2000.4265

31. Ewert S, Honegger A, Plückthun A (2004) Stability improvement of antibodies for extracellular and intracellular applications: CDR grafting to stable frameworks and structure-based framework engineering. Methods 34:184–199. doi: 10.1016/j.ymeth.2004.04.007

32. Kobayashi N, Oyama H (2011) Antibody engineering toward high-sensitivity high-throughput immunosensing of small molecules. Analyst 136:642–651. doi: 10.1039/c0an00603c

33. Vanham G, Bloemmen FJ, Ceuppens JL, Stevens EAM (1984) Influence of serum complement and rheumatoid factor on detection of immune complexes by the C1q and monoclonal rheumatoid factor solid-phase assay. Journal of Immunological Methods 73:301–311. doi: 10.1016/0022-1759(84)90405-8

34. Ylikotila J, Välimaa L, Vehniäinen M, et al. (2005) A sensitive TSH assay in spot-coated microwells utilizing recombinant antibody fragments. Journal of Immunological Methods 306:104–114. doi: 10.1016/j.jim.2005.08.002

35. Hawkins RC (2007) Laboratory Turnaround Time. Clin Biochem Rev 28:179–194.

36. Pelkkikangas A-M, Jaakohuhta S, Lövgren T, Härmä H (2004) Simple, rapid, and sensitive thyroid-stimulating hormone immunoassay using europium(III) nanoparticle label. Analytica Chimica Acta 517:169–176. doi: 10.1016/j.aca.2004.04.043

37. Smith DS, Eremin SA (2008) Fluorescence polarization immunoassays and related methods for simple, high-throughput screening of small molecules. Anal Bioanal Chem 391:1499–1507. doi: 10.1007/s00216-008-1897-z

38. Soukka T, Rantanen T, Kuningas K (2008) Photon Upconversion in Homogeneous Fluorescence-based Bioanalytical Assays. Annals of the New York Academy of Sciences 1130:188–200. doi: 10.1196/annals.1430.027

39. Ekins RP (1997) Immunoassay design and optimisation. Principles and Practice of Immunoassay, 2nd edition. Macmillan, London, pp 173–207

40. Nelson AL (2010) Antibody fragments. MAbs 2:77–83.

41. Demchenko AP (2008) Introduction to Fluorescence Sensing, 2009 edition. Springer, New York

42. Soini E, Hemmilä I (1979) Fluoroimmunoassay: present status and key problems. Clinical Chemistry 25:353–361.

43. Siitari H, Hemmilä I, Soini E, et al. (1983) Detection of hepatitis B surface antigen using time-resolved fluoroimmunoassay. Nature 301:258–260.

44. Haddad PR (1977) The application of ternary complexes to spectrofluorometric analysis. Talanta 24:1–13. doi: 10.1016/0039-9140(77)80177-X

45. Kokko L, Lövgren T, Soukka T (2007) Europium(III)-chelates embedded in nanoparticles are protected from interfering compounds present in assay media. Analytica Chimica Acta 585:17–23. doi: 10.1016/j.aca.2006.12.006

46. Hemmilä I (1985) Fluoroimmunoassays and immunofluorometric assays. Clin Chem 31:359–370.

47. Sapsford KE, Algar WR, Berti L, et al. (2013) Functionalizing Nanoparticles with Biological Molecules: Developing Chemistries that Facilitate Nanotechnology. Chem Rev 113:1904–2074. doi: 10.1021/cr300143v

48. Selby C (1999) Interference in immunoassay. Ann Clin Biochem 36 (Pt 6):704–721.

49. Seydack M (2005) Nanoparticle labels in immunosensing using optical detection methods. Biosensors and Bioelectronics 20:2454–2469. doi: 10.1016/j.bios.2004.11.003

50. Kumar CSSR (2010) Semiconductor Nanomaterials. John Wiley & Sons

51. Beverloo HB, van Schadewijk A, Zijlmans HJ, Tanke HJ (1992) Immunochemical detection of proteins and nucleic acids on filters using small luminescent inorganic crystals as markers. Anal Biochem 203:326–334.

52. Roberts DV, P. Wittmershaus B, Zhang Y-Z, et al. (1998) Efficient excitation energy transfer among multiple dyes in polystyrene microspheres. Journal of Luminescence 79:225–231.

53. Jin Z, Hildebrandt N (2012) Semiconductor quantum dots for in vitro diagnostics and cellular imaging. Trends in Biotechnology 30:394–403. doi: 10.1016/j.tibtech.2012.04.005

54. Hoy J, Morrison PJ, Steinberg LK, et al. (2013) Excitation Energy Dependence of the Photoluminescence Quantum Yields of Core and Core/Shell Quantum Dots. J Phys Chem Lett 4:2053–2060. doi: 10.1021/jz4004735

55. Zheng J, Zhang C, Dickson RM (2004) Highly Fluorescent, Water-Soluble, Size-Tunable Gold Quantum Dots. Phys Rev Lett 93:077402. doi: 10.1103/PhysRevLett.93.077402

56. Joseph D, Geckeler KE (2014) Synthesis of highly fluorescent gold nanoclusters using egg white proteins. Colloids and Surfaces B: Biointerfaces 115:46–50. doi: 10.1016/j.colsurfb.2013.11.017

57. Kricka LJ, Park JY, Li SFY, Fortina P (2005) Miniaturized detection technology in molecular diagnostics. Expert Rev Mol Diagn 5:549–559. doi: 10.1586/14737159.5.4.549

58. Tang D, Cui Y, Chen G (2013) Nanoparticle-based immunoassays in the biomedical field. Analyst 138:981–990. doi: 10.1039/c2an36500f

59. Word JM, Lovell SC, LaBean TH, et al. (1999) Visualizing and quantifying molecular

goodness-of-fit: small-probe contact dots with explicit hydrogen atoms. Journal of Molecular Biology 285:1711–1733. doi: 10.1006/jmbi.1998.2400

60. Sigal GB, Mrksich M, Whitesides GM (1998) Effect of Surface Wettability on the Adsorption of Proteins and Detergents. J Am Chem Soc 120:3464–3473. doi: 10.1021/ja970819l

61. Green NM (1990) Avidin and streptavidin. Meth Enzymol 184:51–67.

62. Puertas S, de Gracia Villa M, Mendoza E, et al. (2013) Improving immunosensor performance through oriented immobilization of antibodies on carbon nanotube composite surfaces. Biosens Bioelectron 43:274–280. doi: 10.1016/j.bios.2012.12.010

63. Leroy P, Devau N, Revil A, Bizi M (2013) Influence of surface conductivity on the apparent zeta potential of amorphous silica nanoparticles. J Colloid Interface Sci 410:81–93. doi: 10.1016/j.jcis.2013.08.012

64. Soukka T, Härmä H, Paukkunen J, Lövgren T (2001) Utilization of kinetically enhanced monovalent binding affinity by immunoassays based on multivalent nanoparticle-antibody bioconjugates. Anal Chem 73:2254–2260.

65. Härmä H, Lehtinen P, Takalo H, Lövgren T (1999) Immunoassay on a single microparticle: the effect of particle size and number on a miniaturized time-resolved fluorometric assay of free prostate-specific antigen. Analytica Chimica Acta 387:11–19. doi: 10.1016/S0003-2670(99)00069-0

66. Klein J (1986) Surface interactions with adsorbed macromolecules. Journal of Colloid and Interface Science 111:305–313. doi: 10.1016/0021-9797(86)90037-8

67. Myszka DG (1999) Improving biosensor analysis. Journal of Molecular Recognition 12:279–284. doi: 10.1002/(SICI)1099-1352(199909/10)12:5<279::AID-JMR473>3.0.CO;2-3

68. Cedervall T, Lynch I, Lindman S, et al. (2007) Understanding the nanoparticle–protein corona using methods to quantify exchange rates and affinities of proteins for nanoparticles. PNAS 104:2050–2055. doi: 10.1073/pnas.0608582104

69. Butler JE (2000) Solid supports in enzyme-linked immunosorbent assay and other solid-phase immunoassays. Methods 22:4–23. doi: 10.1006/meth.2000.1031

70. Boudet F, Thèze J, Zouali M (1991) UV-treated polystyrene microtitre plates for use in an ELISA to measure antibodies against synthetic peptides. J Immunol Methods 142:73–82.

71. Reimhult K, Petersson K, Krozer A (2008) QCM-D analysis of the performance of blocking agents on gold and polystyrene surfaces. Langmuir 24:8695–8700. doi: 10.1021/la800224s

72. Nyilas E, Chiu TH, Herzlinger GA (1974) Thermodynamics of native protein/foreign surface interactions. I. Calorimetry of the human gamma-globulin/glass system. Trans Am Soc Artif Intern Organs 20 B:480–490.

73. Kennel SJ (1982) Binding of monoclonal antibody to protein antigen in fluid phase or bound to solid supports. J Immunol Methods 55:1–12.

74. Hollander Z, Katchalski-Katzir E (1986) Use of monoclonal antibodies to detect conformational alterations in lactate dehydrogenase isoenzyme 5 on heat denaturation and on adsorption to polystyrene plates. Mol Immunol 23:927–933.

75. Butler JE, Ni L, Nessler R, et al. (1992) The physical and functional behavior of capture antibodies adsorbed on polystyrene. Journal of Immunological Methods 150:77–90. doi: 10.1016/0022-1759(92)90066-3

76. Scheuermann J, Viti F, Neri D (2003) Unexpected observation of concentration-dependent dissociation rates for antibody-antigen complexes and other macromolecular complexes in competition experiments. J Immunol Methods 276:129–134.

77. Kricka LJ, Carter TJ, Burt SM, et al. (1980) Variability in the adsorption properties of microtitre plates used as solid supports in enzyme immunoassay. Clinical Chemistry 26:741–744.

78. Ceglarek U, Lembcke J, Fiedler GM, et al. (2004) Rapid simultaneous quantification of immunosuppressants in transplant patients by turbulent flow chromatography combined with tandem mass spectrometry. Clin Chim Acta 346:181–190. doi: 10.1016/j.cccn.2004.03.017

79. Rebeski DE, Winger EM, Shin Y-K, et al. (1999) Identification of unacceptable background caused by non-specific protein adsorption to the plastic surface of 96-well immunoassay plates using a standardized enzyme-linked immunosorbent assay procedure. Journal of Immunological Methods 226:85–92. doi: 10.1016/S0022-1759(99)00051-4

80. Kuningas K, Rantanen T, Karhunen U, et al. (2005) Simultaneous use of time-resolved fluorescence and anti-stokes photoluminescence in a bioaffinity assay. Anal Chem 77:2826–2834. doi: 10.1021/ac048186y

81. Soukka T, Paukkunen J, Härmä H, et al. (2001) Supersensitive Time-resolved Immunofluorometric Assay of Free Prostate-specific Antigen with Nanoparticle Label Technology. Clinical Chemistry 47:1269–1278.

82. Okano K, Takahashi S, Yasuda K, et al. (1992) Using microparticle labeling and counting for attomole-level detection in heterogeneous immunoassay. Analytical Biochemistry 202:120–125. doi: 10.1016/0003-2697(92)90217-U

83. Eriksson S, Vehniäinen M, Jansén T, et al. (2000) Dual-Label Time-resolved Immunofluorometric Assay of Free and Total Prostate-specific Antigen Based on Recombinant Fab Fragments. Clinical Chemistry 46:658–666.

84. Jones SL, Cox JC, Shepherd JM, et al. (1992) Removal of false-positive reactions from plasma in an enzyme immunoassay for bovine interferon-gamma. J Immunol Methods 155:233–240.

85. Kricka LJ (1999) Human Anti-Animal Antibody Interferences in Immunological Assays.

Clinical Chemistry 45:942–956.

86. Eriksson S, Junikka M, Laitinen P, et al. (2003) Negative Interference in Cardiac Troponin I Immunoassays from a Frequently Occurring Serum and Plasma Component. Clinical Chemistry 49:1095–1104. doi: 10.1373/49.7.1095

87. Tate J, Ward G (2004) Interferences in immunoassay. Clin Biochem Rev 25:105–120.

88. De Meyer T, Muyldermans S, Depicker A (2014) Nanobody-based products as research and diagnostic tools. Trends in Biotechnology 32:263–270. doi: 10.1016/j.tibtech.2014.03.001

89. Townsend S, Finlay WJJ, Hearty S, O'Kennedy R (2006) Optimizing recombinant antibody function in SPR immunosensing: The influence of antibody structural format and chip surface chemistry on assay sensitivity. Biosensors and Bioelectronics 22:268–274. doi: 10.1016/j.bios.2006.01.010

90. Kricka LJ (2000) Interferences in Immunoassay—Still a Threat. Clinical Chemistry 46:1037–1038.

91. Preissner CM, O'Kane DJ, Singh RJ, et al. (2003) Phantoms in the Assay Tube: Heterophile Antibody Interferences in Serum Thyroglobulin Assays. The Journal of Clinical Endocrinology & Metabolism 88:3069–3074. doi: 10.1210/jc.2003-030122

92. Nemzek JA, Newcomb DE, Call DR, Remick DG (1999) Plasma interference in an enzyme-linked immunosorbant assay using a commercial matched antibody pair. Immunol Invest 28:209–221.

93. Luzzi VI, Scott MG, Gronowski AM (2003) Negative thyrotropin assay interference associated with an IgGkappa paraprotein. Clin Chem 49:709–710.

94. Weber TH, Käpyaho KI, Tanner P (1990) Endogenous interference in immunoassays in clinical chemistry. A review. Scand J Clin Lab Invest Suppl 201:77–82.

95. Krahn J, Parry DM, Leroux M, Dalton J (1999) High percentage of false positive cardiac troponin I results in patients with rheumatoid factor. Clin Biochem 32:477–480.

96. Glendenning P, Musk AA, Taranto M, Vasikaran SD (2002) Preanalytical factors in the measurement of intact parathyroid hormone with the DPC IMMULITE assay. Clin Chem 48:566–567.

97. Evans MJ, Livesey JH, Ellis MJ, Yandle TG (2001) Effect of anticoagulants and storage temperatures on stability of plasma and serum hormones. Clin Biochem 34:107–112.

98. John R, Henley R, Shankland D (1990) Concentrations of free thyroxin and free triiodothyronine in serum of patients with thyroxin- and triiodothyronine-binding autoantibodies. Clinical Chemistry 36:470–473.

99. Covinsky M, Laterza O, Pfeifer JD, et al. (2000) An IgM lambda antibody to Escherichia coli produces false-positive results in multiple immunometric assays. Clin Chem 46:1157–1161.

100. Lichtenwalner MR, Mencken T, Tully R, Petosa M (1998) False-Positive Immunochemical Screen for Methadone Attributable to Metabolites of Verapamil. Clinical Chemistry 44:1039–1041.

101. Wood WG (1991) "Matrix effects" in immunoassays. Scand J Clin Lab Invest Suppl 205:105–112.

102. Lynch I, Cedervall T, Lundqvist M, et al. (2007) The nanoparticle–protein complex as a biological entity; a complex fluids and surface science challenge for the 21st century. Advances in Colloid and Interface Science 134–135:167–174. doi: 10.1016/j.cis.2007.04.021

103. Arai T, Norde W (1990) The behavior of some model proteins at solid—liquid interfaces 2. Sequential and competitive adsorption. Colloids and Surfaces 51:17–28. doi: 10.1016/0166-6622(90)80128-Q

104. Norde W, Gage D (2004) Interaction of Bovine Serum Albumin and Human Blood Plasma with PEO-Tethered Surfaces: Influence of PEO Chain Length, Grafting Density, and Temperature. Langmuir 20:4162–4167. doi: 10.1021/la030417t

105. Klein J (2007) Probing the interactions of proteins and nanoparticles. PNAS 104:2029–2030. doi: 10.1073/pnas.0611610104

106. Sabatino P, Casella L, Granata A, et al. (2007) Synthetic chrysotile nanocrystals as a reference standard to investigate surface-induced serum albumin structural modifications. Journal of Colloid and Interface Science 314:389–397. doi: 10.1016/j.jcis.2007.05.081

107. Norde W, Giacomelli CE (2000) BSA structural changes during homomolecular exchange between the adsorbed and the dissolved states. Journal of Biotechnology 79:259–268. doi: 10.1016/S0168-1656(00)00242-X

108. Härmä H, Soukka T, Lövgren T (2001) Europium nanoparticles and time-resolved fluorescence for ultrasensitive detection of prostate-specific antigen. Clin Chem 47:561–568.

109. Baumgartner, Hinterdorfer, Schindler (2000) Data analysis of interaction forces measured with the atomic force microscope. Ultramicroscopy 82:85–95.

110. Kienberger F, Ebner A, Gruber HJ, Hinterdorfer P (2006) Molecular recognition imaging and force spectroscopy of single biomolecules. Acc Chem Res 39:29–36. doi: 10.1021/ar050084m

111. Ebner A, Wildling L, Kamruzzahan ASM, et al. (2007) A new, simple method for linking of antibodies to atomic force microscopy tips. Bioconjug Chem 18:1176–1184. doi: 10.1021/bc070030s

112. Lyubchenko YL, Gall AA, Shlyakhtenko LS (2001) Atomic force microscopy of DNA and protein-DNA complexes using functionalized mica substrates. Methods Mol Biol 148:569–578. doi: 10.1385/1-59259-208-2:569

113. Näreoja T, Määttänen A, Peltonen J, et al. (2009) Impact of surface defects and denaturation of capture surface proteins on nonspecific binding in immunoassays using antibody-coated polystyrene nanoparticle labels. J Immunol Methods 347:24–30. doi: 10.1016/j.jim.2009.05.010

114. Riener CK, Stroh CM, Ebner A, et al. (2003) Simple test system for single molecule recognition force microscopy. Analytica Chimica Acta 479:59–75. doi: 10.1016/S0003-2670(02)01373-9

115. Huang GS, Chen Y-S, Yeh H-W (2006) Measuring the Flexibility of Immunoglobulin by Gold Nanoparticles. Nano Lett 6:2467–2471. doi: 10.1021/nl061598x

116. Vaidya HC, Beatty BG (1992) Eliminating interference from heterophilic antibodies in a two-site immunoassay for creatine kinase MB by using F(ab')2 conjugate and polyclonal mouse IgG. Clinical Chemistry 38:1737–1742.

117. Huhtinen P, Pelkkikangas A-M, Jaakohuhta S, et al. (2004) Quantitative, Rapid Europium(III) Nanoparticle-Label-Based All-in-One Dry-Reagent Immunoassay for Thyroid-Stimulating Hormone. Clinical Chemistry 50:1935–1936. doi: 10.1373/clinchem.2004.036962

118. Butler JE, Lü EP, Navarro P, Christiansen B (1997) Comparative studies on the interaction of proteins with a polydimethylsiloxane elastomer. I. Monolayer protein capture capacity (PCC) as a function of protein pl, buffer pH and buffer ionic strength. J Mol Recognit 10:36–51. doi: 10.1002/(SICI)1099-1352(199701/02)10:1<36::AID-JMR353>3.0.CO;2-G

119. Klein JS, Gnanapragasam PNP, Galimidi RP, et al. (2009) Examination of the contributions of size and avidity to the neutralization mechanisms of the anti-HIV antibodies b12 and 4E10. PNAS 106:7385–7390. doi: 10.1073/pnas.0811427106

120. Kuzuya A, Numajiri K, Kimura M, Komiyama M (2008) Single-molecule accommodation of streptavidin in nanometer-scale wells formed in DNA nanostructures. Nucleic Acids Symp Ser (Oxf) 681–682. doi: 10.1093/nass/nrn344

121. Näreoja T, Vehniäinen M, Lamminmäki U, et al. (2009) Study on nonspecificity of an immuoassay using Eu-doped polystyrene nanoparticle labels. J Immunol Methods 345:80–89. doi: 10.1016/j.jim.2009.04.008

122. Schwesinger F, Ros R, Strunz T, et al. (2000) Unbinding forces of single antibody-antigen complexes correlate with their thermal dissociation rates. Proc Natl Acad Sci USA 97:9972–9977.

123. Ikai A, Afrin R (2003) Toward mechanical manipulations of cell membranes and membrane proteins using an atomic force microscope: an invited review. Cell Biochem Biophys 39:257–277. doi: 10.1385/CBB:39:3:257

124. Ratto TV, Langry KC, Rudd RE, et al. (2004) Force spectroscopy of the double-tethered concanavalin-A mannose bond. Biophys J 86:2430–2437. doi: 10.1016/S0006-3495(04)74299-X

125. Wakayama J, Sekiguchi H, Akanuma S, et al. (2008) Methods for reducing nonspecific interaction in antibody-antigen assay via atomic force microscopy. Anal Biochem 380:51–58. doi: 10.1016/j.ab.2008.05.036

126. Merkel R, Nassoy P, Leung A, et al. (1999) Energy landscapes of receptor-ligand bonds explored with dynamic force spectroscopy. Nature 397:50–53. doi: 10.1038/16219

127. Fujiki T, Tsuji A, Matsumoto S, et al. (2010) Generation of a human anti-tumor necrosis factor-α monoclonal antibody by in vitro immunization with a multiple antigen peptide. Biosci Biotechnol Biochem 74:1836–1840.

128. Brockmann E-C, Lamminmäki U, Saviranta P (2005) Engineering dihydropteroate synthase (DHPS) for efficient expression on M13 phage. Biochimica et Biophysica Acta (BBA) - General Subjects 1724:146–154. doi: 10.1016/j.bbagen.2005.04.012

129. Rankl C, Kienberger F, Wildling L, et al. (2008) Multiple receptors involved in human rhinovirus attachment to live cells. Proc Natl Acad Sci USA 105:17778–17783. doi: 10.1073/pnas.0806451105

130. Kusnezow W, Syagailo YV, Rüffer S, et al. (2006) Optimal Design of Microarray Immunoassays to Compensate for Kinetic Limitations Theory and Experiment. Mol Cell Proteomics 5:1681–1696. doi: 10.1074/mcp.T500035-MCP200

131. Kusnezow W, Syagailo YV, Rüffer S, et al. (2006) Kinetics of antigen binding to antibody microspots: strong limitation by mass transport to the surface. Proteomics 6:794–803. doi: 10.1002/pmic.200500149

132. Patil-Sisodia K, Mestman JH (2010) Graves hyperthyroidism and pregnancy: a clinical update. Endocr Pract 16:118–129. doi: 10.4158/EP09233.RA

133. Alexander EK, Marqusee E, Lawrence J, et al. (2004) Timing and Magnitude of Increases in Levothyroxine Requirements during Pregnancy in Women with Hypothyroidism. New England Journal of Medicine 351:241–249. doi: 10.1056/NEJMoa040079

134. Reinehr T (2010) Obesity and thyroid function. Mol Cell Endocrinol 316:165–171. doi: 10.1016/j.mce.2009.06.005

135. Nyrnes A, Jorde R, Sundsfjord J (2005) Serum TSH is positively associated with BMI. Int J Obes Relat Metab Disord 30:100–105. doi: 10.1038/sj.ijo.0803112

136. Sari R, Balci MK, Altunbas H, Karayalcin U (2003) The effect of body weight and weight loss on thyroid volume and function in obese women. Clinical Endocrinology 59:258–262. doi: 10.1046/j.1365-2265.2003.01836.x

137. Kershaw EE, Flier JS (2004) Adipose tissue as an endocrine organ. J Clin Endocrinol Metab 89:2548–2556. doi: 10.1210/jc.2004-0395

138. Diamant S, Gorin E, Shafrir E (1972) Enzyme activities related to fatty-acid synthesis in liver and adipose tissue of rats treated with triiodothyronine. Eur J Biochem 26:553–559.